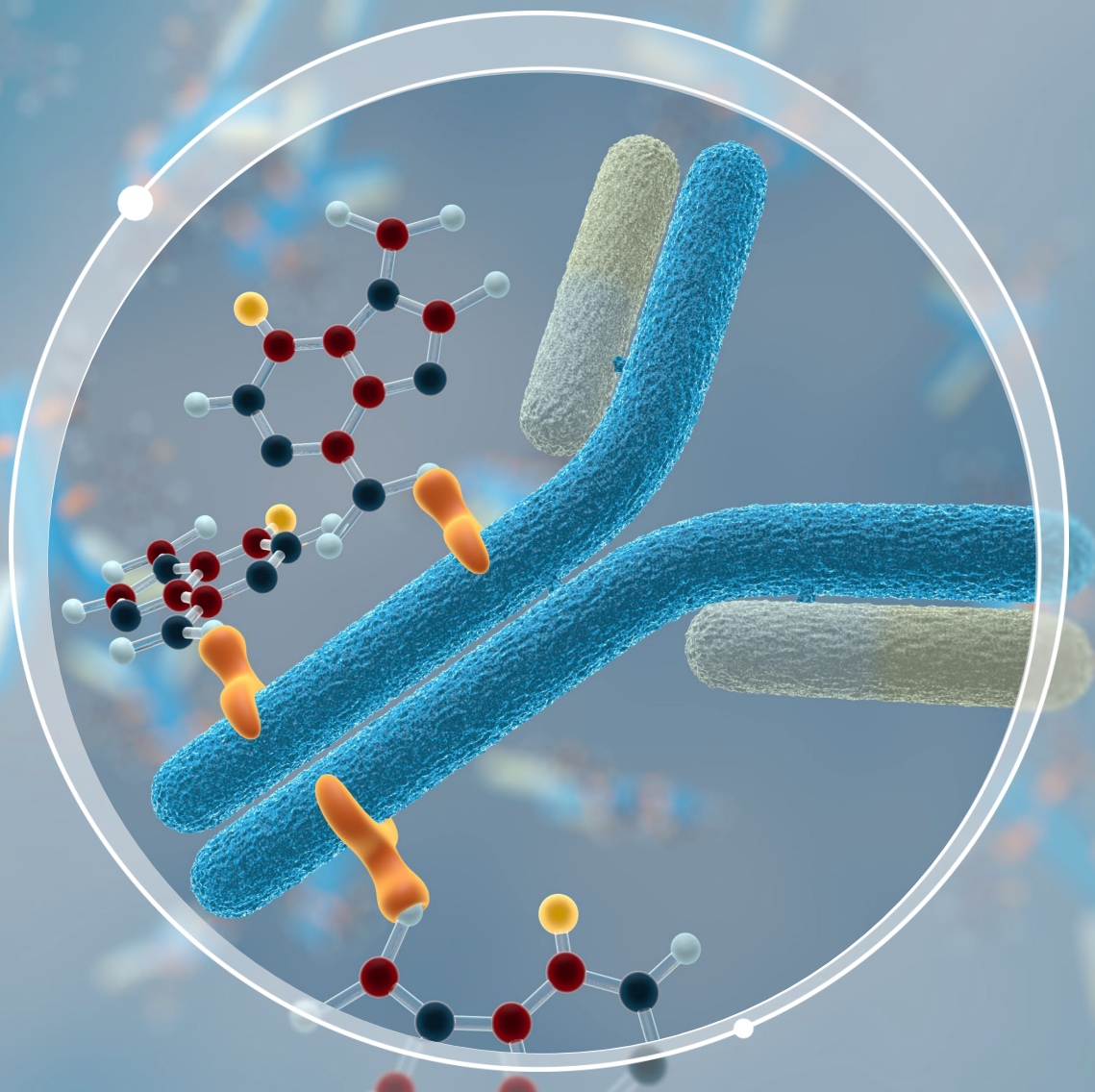


2023 生物製藥應用文集

抗體藥物複合體 (ADC)



目錄

- 1. 使用電子活化解離(EAD)工作流程實現具高序列覆蓋度和可信度的生物治療藥物雙硫鍵圖譜 (Achieving ultrahigh sequence coverage and high-confidence disulfide bond mapping of biotherapeutics using an electron-activated dissociation (EAD)-based middle-down workflow)**
 - 透過EAD對於雙硫鍵的特異性碎裂以獲得具高覆蓋率和可信度的抗體亞基鑑定圖譜
- 2. 使用電子活化解離 (EAD) 技術全面性鑑定抗體藥物複合體(ADC) (Comprehensive characterization of an antibody-drug conjugate (ADC) using electron activated dissociation (EAD))**
 - 基於EAD 技術的胜肽圖譜鑑定工作流程能在單次進樣中對複雜ADC進行全面鑑定
- 3. 使用碰撞誘導解離 (CID) 和電子活化解離 (EAD) 增強胜肽圖譜鑑定的單次進樣工作流程 (A single-injection workflow for enhanced peptide mapping using collision-induced dissociation (CID) and electron-activated dissociation (EAD))**
 - 單次進樣的CID/EAD DDA 工作流程結合了CID和EAD技術的優勢，提供生物治療藥物的全面性鑑定
- 4. 用於確認抗體藥物複合體 (ADC) 的藥物抗體比率 (DAR) 的簡易工作流程 (A streamlined workflow for the determination of the drug-to-antibody ratio (DAR) of antibody-drug conjugates (ADCs))**
 - 透過Zeno TOF 7600系統對 ADC 進行精確質量測量，並整合軟體進行自動化DAR 計算
- 5. 使用電子活化解離 (EAD) 進行生物治療藥物鑑定的簡易單針進樣工作流程 (A streamlined single-injection middle-down workflow using electron-activated dissociation (EAD) for biotherapeutics characterization)**
 - 透過從EAD的碎裂中檢測到的特異性碎片，Fc/2 和 Fd 亞基的 PTM 得到了可靠的鑑定
- 6. 針對特定等電點範圍的多種完整單株抗體進行直接、快速的多重屬性監測 (Direct and rapid multi-attribute monitoring of multiple intact monoclonal antibodies with a wide isoelectric-point range of 7.3 to 9.1)**
 - Intabio ZT 系統可實現簡易工作流程，透過 icIEF 分離電荷異構物，並使用 ZenoTOF 7600 系統在 7.3 至 9.1 的 pI 範圍內進行識別
- 7. 用於生物治療藥物高通量分析的CE-SDS工作流程 (Lightning capillary electrophoresis sodium dodecyl sulfate (CE-SDS) workflow for high-throughput analysis of biotherapeutics)**
 - 透過快速的CE-SDS工作流程可以提升1.5倍分析速度且具有良好穩定性及準確度

Achieving ultrahigh sequence coverage and high-confidence disulfide bond mapping of biotherapeutics using an electron-activated dissociation (EAD)-based middle-down workflow

Featuring the EAD-based middle-down workflow using the ZenoTOF 7600 system and Biologics Explorer software from SCIEX

Haichuan Liu¹, Rashmi Madda¹, Andy Mahan², Hirsh Nanda², Wen Jin³, Pavel Ryumin³ and Zoe Zhang¹
¹SCIEX, USA; ²Janssen, USA; ³SCIEX, Canada

This technical note highlights an innovative EAD-based middle-down workflow for achieving ultrahigh sequence coverages (85%-93%) of antibody subunits. Additionally, this workflow provides valuable insights into the intra-chain disulfide linkages. The combination of complementary EAD results from the fully reduced and disulfide-linked subunits led to ultrahigh sequence coverage of antibody subunits in 2 injections in addition to high-confidence disulfide bond mapping.

Middle-down mass spectrometry (MS) is emerging as a promising approach for biotherapeutic characterization.¹⁻⁵ Middle-down MS provides much higher sequence coverage of biotherapeutics than top-down MS. Compared to bottom-up MS, middle-down MS benefits from simpler sample preparation, a lower degree of artificial modification, easier data interpretation, fewer false positive identifications and higher throughput. One of the limitations of traditional middle-down workflows is the lack of fragmentation in the middle of a subunit sequence. This limitation can be overcome by applying EAD to disulfide-linked subunits.⁵

The state-of-the-art, EAD-based middle-down workflow combines accurate mass measurement and information-rich

EAD fragmentation with automated data analysis for rapid sequence confirmation, accurate PTM localization and high-confidence disulfide bond mapping.¹⁻⁵ In this technical note, these powerful capabilities of EAD were leveraged to provide a nearly complete sequence coverage of antibody subunits and high-confidence disulfide bond mapping (Figure 1).

Key features of the EAD-based middle-down workflow for biotherapeutic characterization

- **Ultrahigh sequence coverage:** The combined EAD results for the fully reduced and disulfide-linked subunits provide 85%-93% sequence coverage of antibody subunits
- **High-confidence disulfide bond mapping:** EAD leads to a distinctive fragmentation pattern of disulfide-linked subunits for rapid disulfide bond mapping with minimal false positives
- **Accurate localization of PTMs:** Labile PTMs are preserved in the EAD fragments for their accurate localization
- **Streamlined and easy to implement:** The workflow requires minimal method optimization and is streamlined from data acquisition to results review

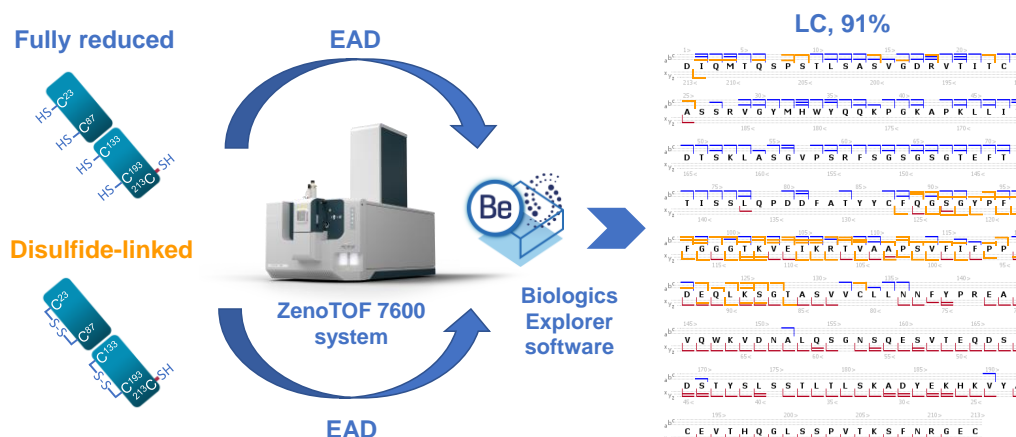


Figure 1. EAD-based middle-down analysis of the fully reduced and disulfide-linked antibody subunits led to a nearly complete sequence coverage (85%-93%) of antibody subunits in 2 injections. EAD provided high sequence coverage (70%-85%) of the fully reduced mAb subunits in a single injection.¹⁻⁴ The characteristic fragmentation of the disulfide-linked subunits by EAD led to the detection of unique fragments from the middle of the sequence between 2 central Cys residues, as highlighted by the orange lines in the coverage map.⁵ The addition of these fragments offered a significant increase in sequence coverage and provided high-confidence mapping of the intra-chain disulfide bonds.

Methods

Sample preparation: The details of sample preparation for the fully reduced and disulfide-linked subunits of NISTmAb, bevacizumab, trastuzumab and a trisppecific antibody (tsAb) were described in previous technical notes.¹⁻⁵ Briefly, to prepare the fully reduced subunits, the antibody samples were incubated with FabRICATOR (IdeS) from Genovis at 37°C for 2 hours, then were denatured using guanidine hydrochloride (GuHCl) and reduced at 60°C for 30 minutes using dithiothreitol (DTT). The disulfide-linked subunits were prepared by incubating the IdeS-treated antibodies with DTT at 37°C for 15 minutes in the absence of GuHCl. Finally, 1-5 μ L of the final solution (1-2 μ g) was injected for LC-MS analysis.

Chromatography: The subunits of NISTmAb and tsAb were separated using an ACQUITY UPLC Protein BEH C4 column (2.1 \times 50 mm, 1.7 μ m, 300 \AA , Waters). The LC gradients used for the subunit separation are shown in Table 1. A flow rate of 0.3 mL/min was used for all LC runs. The column was kept at 60°C in the column oven of an ExionLC system (SCIEX). Mobile phase A was 0.1% formic acid in water and mobile phase B was 0.1% formic acid in acetonitrile.

Table 1. LC gradient for subunit separation.

Time (min)	A (%)	B (%)
Initial	80	20
2	80	20
14	65 or 60	35 or 40
15	10	90
17	10	90
17.5	80	20
20	80	20

Mass spectrometry: MRM^{HR} EAD experiments were performed in SCIEX OS software using the ZenoTOF 7600 system. 1-3 charge states were targeted for EAD fragmentation of the fully reduced and disulfide-linked subunits. The key TOF MS and MRM^{HR} settings used are listed in Tables 2 and 3, respectively.

Data processing: MRM^{HR} data were analyzed using a middle-down workflow template in Biologics Explorer software.

Table 2. TOF MS parameters.

Parameter	Value
Spray voltage	5500 V
TOF start mass	500 m/z
TOF stop mass	3000 m/z
Accumulation time	0.1 s
Source temperature	400°C
Declustering potential	80 V
Collision energy	10 V
Time bins to sum	8

Table 3. MRM^{HR} parameters using EAD.

Parameter	Value
Start mass	100 m/z
Stop mass	3000-5000 m/z
Q1 resolution	Low
Zeno trap	ON
Zeno threshold	100,000 cps
Accumulation time	0.1 or 0.2 s
Declustering potential	80 V
CE	12 V
Time bins to sum	8
Electron beam current	5000 nA
Electron KE	1 eV
ETC	100%
Reaction time	5 or 10 ms
EAD RF	150 Da

EAD of the fully reduced and disulfide-linked antibody subunits

The EAD-based middle-down workflow provides consistently high sequence coverages (70%-85%) and accurate localization of PTMs for the fully reduced antibody subunits.¹⁻⁴ For the disulfide-linked subunits, EAD leads to a characteristic fragmentation pattern in which the bond cleavages occur primarily outside the disulfide-forming regions, enabling rapid disulfide bond mapping of biotherapeutics on the subunit level with high confidence and high fidelity.⁵ The combination of complementary EAD results of the fully reduced and disulfide-linked subunits offers an innovative strategy to achieve a nearly complete characterization of biotherapeutics with minimal modification artifacts and false positives.

Figure 2 compares the EAD MS/MS spectra of the fully reduced and disulfide-linked LC subunit of bevacizumab. EAD led to excellent fragmentation and information-rich spectra in both cases. However, a distinctive difference was observed between EAD fragmentation of the fully reduced and disulfide-linked subunits. EAD of the fully reduced LC subunit resulted in an

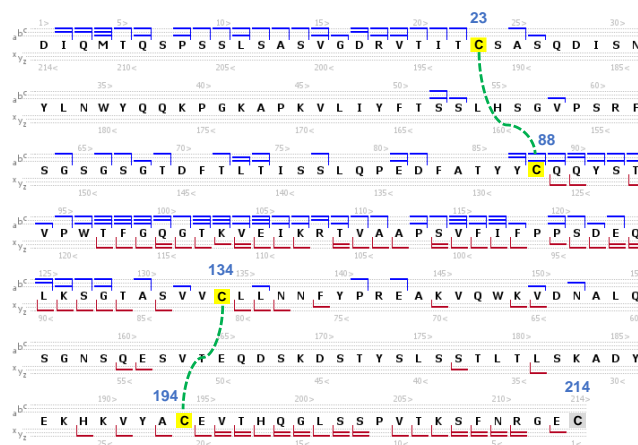


Figure 3. Sequence coverage map of the disulfide-linked LC subunit from bevacizumab. EAD led to the formation of fragments predominantly from outside the 2 disulfide-forming regions between Cys²³-Cys⁸⁸ and Cys¹³⁴-Cys¹⁹⁴, confirming the expected intra-chain disulfide linkages in this subunit. The C-terminal Cys²¹⁴ residue was present in its reduced form.

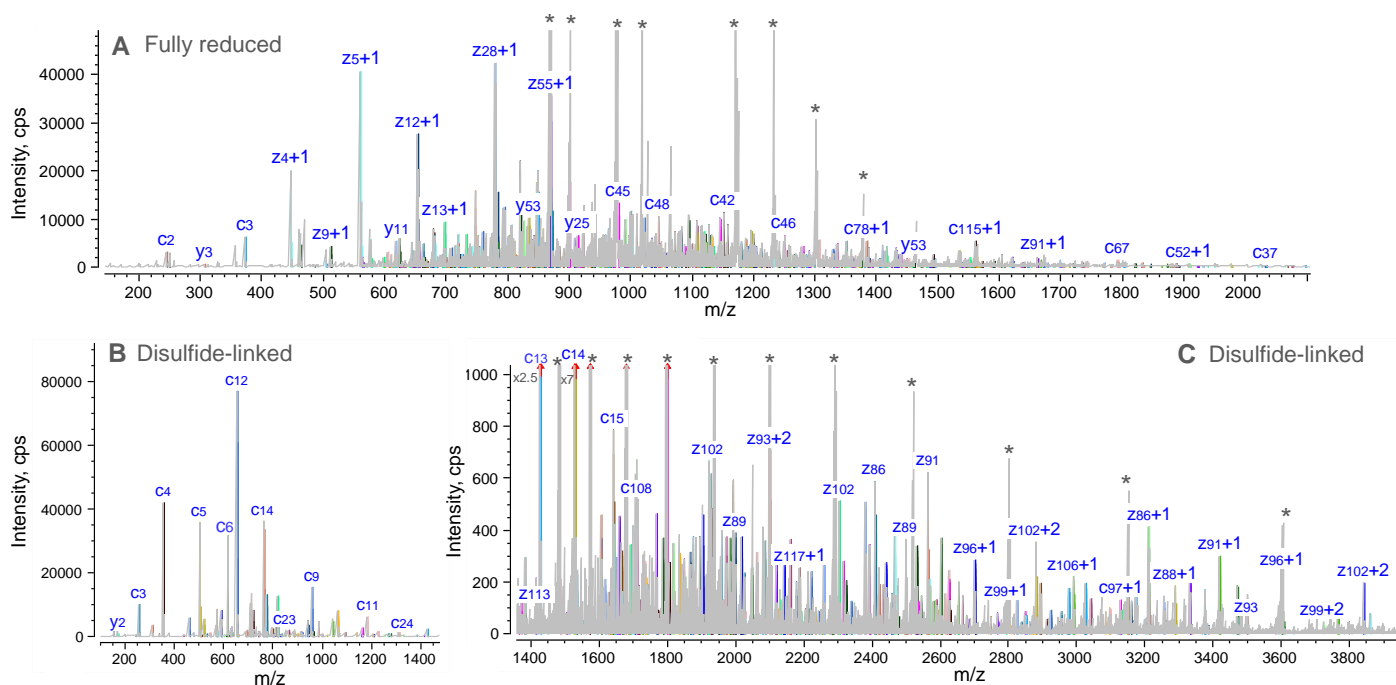


Figure 2. Annotated EAD MS/MS spectra of the fully reduced and disulfide-linked LC subunit of bevacizumab from Biologics Explorer software. The EAD spectrum of the fully reduced LC subunit is displayed in the full m/z range of ~150-2,100 (A), whereas the EAD spectrum of the disulfide-linked subunit is shown in 2 different m/z ranges of ~150-1,400 (B) and ~1,400-3,850 (C) for a better spectral view. EAD provided excellent fragmentation and information-rich MS/MS spectra for the fully reduced and disulfide-linked LC subunits. Complementary results were obtained from the 2 experiments. EAD of the fully reduced subunit led to extensive fragmentation of the N- and C-terminal regions, with limited cleavages in the middle of the sequence. By comparison, EAD fragmentation of the disulfide-linked subunit occurred primarily outside the disulfide-forming regions, including the central region between the Cys⁸⁸ and Cys¹³⁴ residues in the LC subunit of bevacizumab, leading to the detection of rich large c/z fragments across the high m/z range (C). Not all fragments are displayed for spectral clarity. The peaks labeled with asterisks are the precursors or charge-reduced species.

extensive fragmentation across the N- and C-terminal regions of the sequence, producing a relatively even distribution of the fragments across the m/z range of ~400-1600 (Figure 2A). By comparison, EAD fragmentation of the disulfide-linked LC subunit was concentrated on the sequences outside the 2 disulfide-forming regions. This led to the detection of the low m/z fragments from the 2 termini (Figure 2B and Figure 3) and rich high m/z fragments from the central region between the Cys⁸⁸ and Cys¹³⁴ residues (Figure 2C and Figure 3). This characteristic fragmentation pattern of the disulfide-linked subunits allowed confident confirmation of the intra-chain disulfide bonds in the LC subunit of bevacizumab (Figure 3). In this technical note, the complementary EAD results of the fully reduced and disulfide-linked subunits were leveraged to achieve a nearly complete sequence coverage of biotherapeutics in 2 injections.

Achieving ultrahigh sequence coverage of biotherapeutics

As mentioned above, EAD resulted in complementary fragmentation of the fully reduced and disulfide-linked subunits of biotherapeutics. EAD of the disulfide-linked subunits led to extensive fragmentation of the middle of the sequence, a region that is challenging to cleave in the fully reduced subunits. As a result, many unique bond cleavages were detected in EAD of the

disulfide-linked subunits. The combination of these cleavages with those detected by EAD of the fully reduced subunits led to an ultrahigh sequence coverage of antibody subunits in 2 injections.

Figure 4 and 5 show the sequence coverage maps of the LC, Fd and Fc/2 subunits from NISTmAb and bevacizumab, respectively, based on the combined EAD results of the fully reduced and disulfide-linked subunits. An ultrahigh sequence coverage of $\geq 90\%$ was achieved for all subunits except the NISTmAb Fd subunit, for which 85% sequence coverage was obtained. The unique bond cleavages detected by EAD of the disulfide-linked subunits, as highlighted by the orange lines in Figure 4 and 5, contributed to an absolute increase of 10%-16% in sequence coverage. Ultrahigh sequence coverages were also obtained for the LC (92%), Fd (90%) and Fc/2 (88%) subunits of trastuzumab (data not shown).

Figure 6 shows the combined sequence coverage of a tsAb LC subunit from 2 EAD experiments. Similar to the results described above, EAD of the disulfide-linked LC subunit of the tsAb contributed to an absolute increase in sequence coverage by ~10%, leading to an ultrahigh sequence coverage (88%) of the tsAb LC subunit.

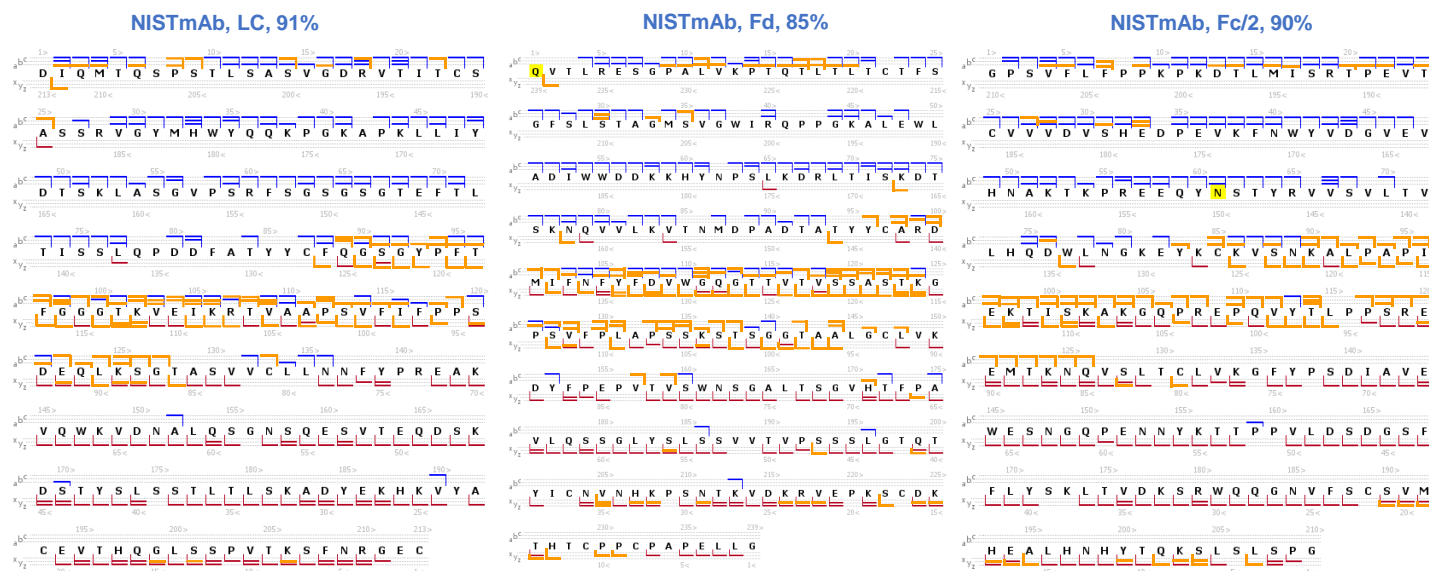


Figure 4. The combined sequence coverage maps of NISTmAb LC, Fd and Fc/2 subunits from 2 EAD injections. EAD of the fully reduced NISTmAb LC, Fd and Fc/2 subunits led to 70%-80% sequence coverage of the 3 subunits in a single injection.¹ The corresponding bond cleavages are indicated by the blue and red lines in the 3 sequence coverage maps. The distinctive EAD fragmentation patterns of the disulfide-linked subunits enabled the detection of many unique fragments from the regions not restricted by the disulfide bonds, including the middle of the sequence. These unique fragments are highlighted by the orange lines in the 3 coverage maps. The combined EAD results from the 2 injections led to 85%-91% sequence coverage of the 3 NISTmAb subunits, with an absolute increase of ~10%-16% contributed by unique fragments produced from EAD of the disulfide-linked subunits. The N-terminal glutamine residue highlighted in the sequence of the Fd subunit (middle panel) was converted into a pyroglutamic acid. The Asn residue highlighted in the sequence of the Fc/2 subunit (right panel) was modified with a G0F glycan.

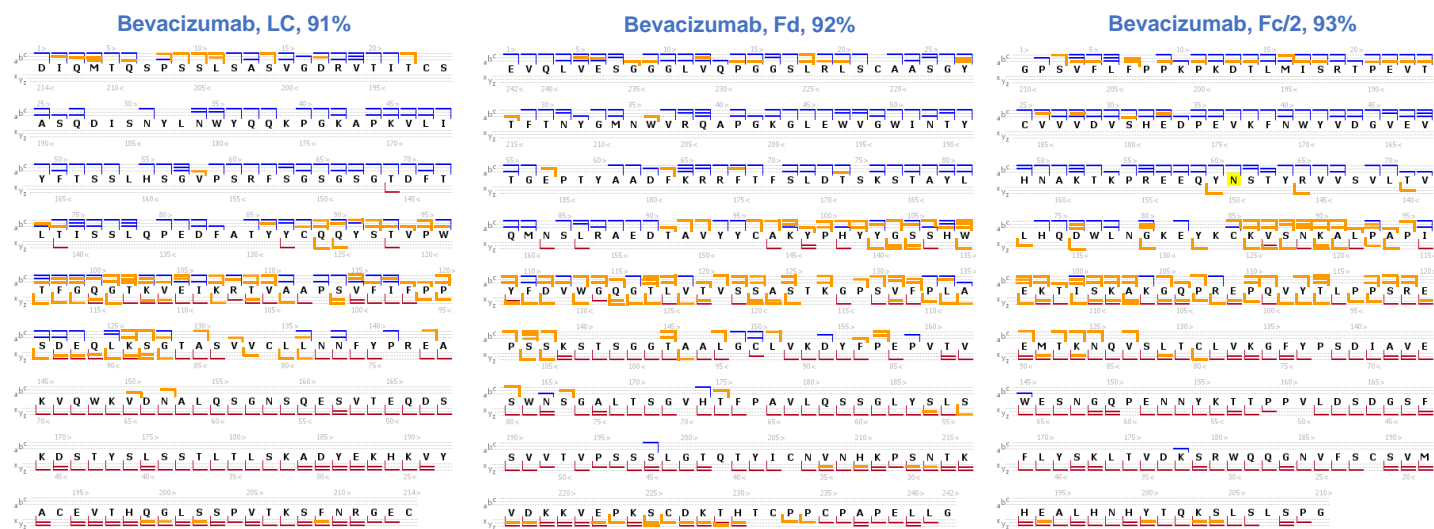


Figure 5. The combined sequence coverage maps of bevacizumab LC, Fd and Fc/2 subunits from 2 EAD injections. The combined EAD results for the fully reduced and disulfide-linked subunits from 2 injections led to >90% sequence coverage of the 3 bevacizumab subunits. The unique fragments produced from EAD of the disulfide-linked subunits, as highlighted by the orange lines in the 3 coverage maps, contributed to a ~10-16% increase in the sequence coverage. The Asn residue highlighted in the sequence of the Fc/2 subunit carried a G0F glycan.

In addition to providing unique bond cleavages, EAD of the disulfide-linked subunits offered rapid disulfide bond mapping and confirmation of the N- and C-terminal cleavages detected by EAD of the fully reduced subunits. These benefits significantly improved confidence in antibody sequence characterization.

In summary, the innovative EAD-based middle-down strategy described in this technical note led to ultrahigh sequence coverage (85%-93%) of biotherapeutics in 2 injections by leveraging the complementary EAD results of the fully reduced and disulfide-linked subunits. This powerful strategy also enabled high-confidence disulfide bond mapping at the subunit level based on the EAD results for the disulfide-linked subunits. This innovative middle-down strategy provides a balanced approach for the comprehensive characterization of biotherapeutics by overcoming the shortcomings of top-down MS in fragmentation efficiency and sequence coverage, and the limitations of bottom-up MS in modification artifacts, data complexity, false positives and throughput. The strategy can greatly improve the efficiency and effectiveness of middle-down MS for the comprehensive characterization of biotherapeutics.

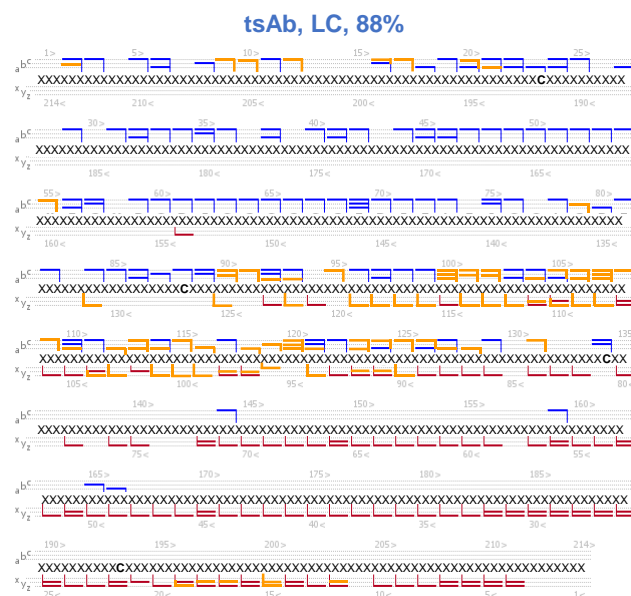


Figure 6. The combined sequence coverage map of the LC subunit of the tsAb. The unique cleavages detected by EAD of the disulfide-linked subunit, as highlighted by the orange lines, contributed to a 10% increase in sequence coverage.

Conclusions

- An innovative EAD-based middle-down MS strategy led to ultrahigh sequence coverages (85%-93%) for antibody subunits in 2 injections
- The characteristic fragmentation pattern offered by EAD for the disulfide-linked subunits enabled rapid disulfide bond mapping with high confidence and high fidelity
- Complementary fragmentation was achieved from EAD of the fully reduced and disulfide-linked subunits
- The powerful strategy provides an in-depth characterization of fully or partially reduced biotherapeutics
- Biologics Explorer software offers easy-to-use middle-down workflow templates and powerful visualization tools for improved user experience with data analysis

References

1. A streamlined single-injection middle-down workflow using electron activated dissociation (EAD) for biotherapeutics characterization. [SCIEX technical note, MKT-26997-A](#).
2. Obtaining high sequence coverage and confident post-translational modification (PTM) analysis of biotherapeutics using an electron activated dissociation (EAD)-based middle-down workflow. [SCIEX technical note, MKT-27223-A](#).
3. Comparative analysis of biotherapeutics using an electron-activated dissociation (EAD)-based middle-down workflow. [SCIEX technical note, MKT-27427-A](#).
4. Confident sequence analysis of a trispecific antibody using an electron-activated dissociation (EAD)-based middle-down workflow. [SCIEX technical note, MKT-27784-A](#).
5. High-confidence disulfide bond mapping of biotherapeutics using an electron-activated dissociation (EAD)-based middle-down workflow. [SCIEX technical note, MKT-28341-A](#).

The SCIEX clinical diagnostic portfolio is For In Vitro Diagnostic Use. Rx Only. Product(s) not available in all countries. For information on availability, please contact your local sales representative or refer to www.sciex.com/diagnostics. All other products are For Research Use Only. Not for use in Diagnostic Procedures.

Trademarks and/or registered trademarks mentioned herein, including associated logos, are the property of AB Sciex Pte. Ltd. or their respective owners in the United States and/or certain other countries (see www.sciex.com/trademarks).

© 2023 DH Tech. Dev. Pte. Ltd. MKT-28565-A



Headquarters
500 Old Connecticut Path | Framingham, MA 01701 USA
Phone 508-383-7700
sciex.com

International Sales
For our office locations please call the division headquarters or refer to our website at sciex.com/offices

Comprehensive characterization of an antibody-drug conjugate (ADC) using electron activated dissociation (EAD)

Featuring an EAD-based peptide mapping workflow using the ZenoTOF 7600 system and Biologics Explorer software from SCIEX

Zoe Zhang¹, Haichuan Liu¹, Takashi Baba², Pavel Ryumin², Bill Loyd², Jason Causon² and Kerstin Pohl¹
¹SCIEX, USA; ²SCIEX, Canada

This technical note describes an in-depth characterization of a lysine-linked ADC using a streamlined, EAD-based peptide mapping workflow in a single injection. This workflow combines the powerful capabilities of EAD for peptide mapping with automated data interpretation offered by Biologics Explorer software. The workflow provides confident ADC sequence confirmation and accurate localization of the payload. The EAD-based peptide mapping workflow involves minimal method development and optimization, allowing its easy implementation by different levels of users.

Traditional collision-based tandem mass spectrometry (MS/MS) approaches lead to fragmentation of the cytotoxic payload in the ADC. Often CID does not provide site-specific information critical to biotherapeutic development. Although conventional electron-based MS/MS approaches can provide site information about the payload, these techniques suffer from slow scan rates, long reaction times, low sensitivity and low reproducibility. By comparison, EAD can be implemented as a data-dependent acquisition (DDA) platform method for comprehensive biotherapeutic characterization with high sensitivity and high reproducibility.¹⁻³

In this technical note, the EAD-based peptide mapping workflow (Figure 1) was leveraged to provide complete sequence coverage and accurate localization of the payload in ado-trastuzumab emtansine (T-DM1) in a single injection.

Key features of the ZenoTOF 7600 system for ADC characterization

- **New depth in peptide mapping analysis:** The EAD DDA platform method enables comprehensive analysis of monoclonal antibodies (mAbs) and ADCs in a single injection
- **Confident payload localization and characterization:** EAD provides information for accurate localization and detailed structural characterization of the payload
- **High MS/MS sensitivity:** The Zeno trap improves the detection of fragments by 5- to 10-fold, enabling higher confidence in fragment assignment and peptide identification
- **High quality and reproducibility:** Excellent fragmentation reproducibly with EAD improves confidence in the results
- **Streamlined and easy-to-use:** Automated interpretation of EAD DDA data using Biologics Explorer software allows for easy method implementation and improved user experience

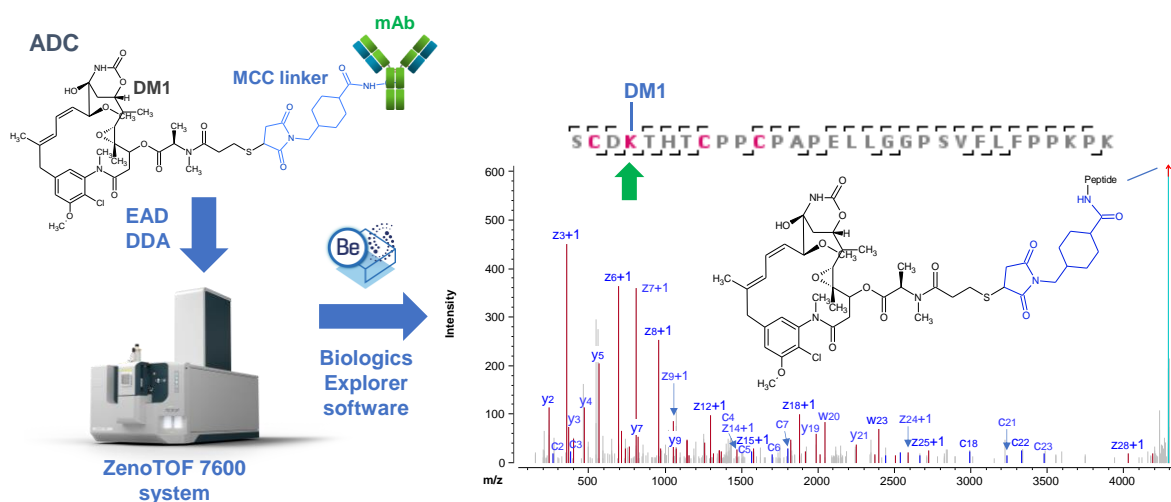


Figure 1. The EAD-based peptide mapping workflow offered by the ZenoTOF 7600 system enables confident sequence confirmation and accurate determination of the payload conjugate sites in T-DM1. The cytotoxic payload, DM1, was retained in the EAD fragments, leading to its accurate localization in the ADC using Biologics Explorer software. MCC: maleimidomethyl cyclohexane-1-carboxylate.

Introduction

With advancements in protein engineering, antibodies and ADCs have become an important class of biotherapeutics.³ ADCs are typically composed of a ~150 kDa mAb covalently coupled with a cytotoxic payload through synthetic linkers.⁴ ADCs have more complex structures and higher sample heterogeneity compared to unconjugated mAbs because the variants carry different numbers of the payload at different conjugation sites.⁵ As a result, it is critical to fully characterize ADCs during their development to ensure drug quality, safety and efficacy. Comprehensive characterization of ADCs typically involves confirmation of the mAb sequence, identification and localization of post-translational modifications (PTMs) on the mAb, measurement of the drug-to-antibody ratio (DAR) and determination of payload conjugation sites. While intact mass analysis is commonly utilized to determine the DAR, sequence confirmation and localization of the payload are typically achieved using a bottom-up approach.

Methods

Sample preparation: T-DM1 was denatured with 7.2M guanidine hydrochloride (HCl) in 100mM Tris-HCl buffer (pH = 7.2), followed by reduction with 10mM DL-dithiothreitol and alkylation using 30mM iodoacetamide. Digestion was performed with the trypsin/Lys-C protease at 37°C for 16 h.

Chromatography: A 4 μ L (4 μ g) sample of the trypsin/Lys-C digest was separated with a CSH C18 column (2.1 \times 100 mm, 1.7 μ m, 130 Å, Waters) using an ExionLC AD system. Mobile phase A was water with 0.1% formic acid and mobile phase B was

Table 1. Chromatography for peptide mapping analysis.

Time (min)	Mobile phase A (%)	Mobile phase B (%)
Initial	98	2
5	98	2
6	90	10
40	55	45
44	10	90
46	10	90
47	98	2
50	98	2
51	10	90
54	10	90
55	98	2
60	98	2

acetonitrile with 0.1% formic acid. Table 1 shows the LC gradient used for peptide separation at a 300 μ L/min flow rate. The column temperature was maintained at 50°C in the column compartment.

Mass spectrometry: EAD DDA data were acquired using SCIEX OS software on the ZenoTOF 7600 system (SCIEX). Detailed TOF MS and EAD DDA method parameters are summarized in Table 2.

Table 2. MS parameters.

Parameter	MS	MS/MS
Scan mode	TOF-MS	DDA
Polarity		Positive
Gas 1		40 psi
Gas 2		40 psi
Curtain gas		30 psi
Source temperature		350°C
Ion spray voltage		5,200 V
Declustering potential		20 V
Collision energy		8 V
CAD gas		7
Maximum candidate ion		5
Intensity threshold		100 cps
Charge states		2 to 10
Exclusion time		6 s after 2 occurrences
Start mass	100 m/z	150 m/z
Stop mass	1,800 m/z	2,500 m/z
Electron KE	NA	7 eV
Electron beam current	NA	4,750 nA
ETC	NA	100
Zeno trap	NA	ON
Accumulation time	0.25 s	0.20 s
Time bins to sum	4	4

Data processing: EAD DDA data were processed using the peptide mapping workflow template within Biologics Explorer software. The combination of DM1 and the maleimidomethyl cyclohexane-1-carboxylate (MCC) linker was defined as a variable modification for the protein N-terminus and lysine (K) residue.

Peptide mapping analysis of T-DM1

T-DM1 was approved in 2013 by the U.S. Food and Drug Administration (FDA) for the treatment of human epidermal growth factor receptor 2 (HER2)-positive, metastatic breast cancer.^{5,6} T-DM1 is composed of trastuzumab covalently conjugated to the cytotoxin DM1 via a non-cleavable MCC linker, which is connected to the primary amine of the protein N-terminal or lysine residue (Figure 2). Previous intact mass studies showed that the average DAR for T-DM1 is ~3.5.^{5,6} Considering that trastuzumab contains 88 lysine and 4 N-terminal residues, the addition of DM1 to these potential conjugation sites may result in >4.5 million possible variants of the T-DM1.⁵ Since the structure and conjugation site of the payload can impact drug safety and efficacy, it is important to confidently identify the payload-containing peptides and accurately determine the sites of payload conjugation.

Peptide mapping is the method of choice for providing simultaneous identification of payload-containing peptides and localization of the payload. Traditional collision-induced dissociation (CID) of DM1-containing peptides resulted in the preferable fragmentation of the payload, leading to the formation of small fragments such as *m/z* 547.2, 485.2 and 453.2.⁵ This fragmentation pattern increases the spectral complexity and ambiguity of the payload localization. This work employed the EAD-based peptide mapping workflow to obtain confident sequence confirmation and precise localization of the DM1 payload in T-DM1. This powerful workflow leverages the unique capabilities of EAD for the preservation of labile PTMs and automated data analysis using Biologics Explorer software, leading to comprehensive ADC characterization in a single injection.

The EAD-based peptide mapping workflow benefited from the excellent fragmentation and high sensitivity of Zeno EAD to

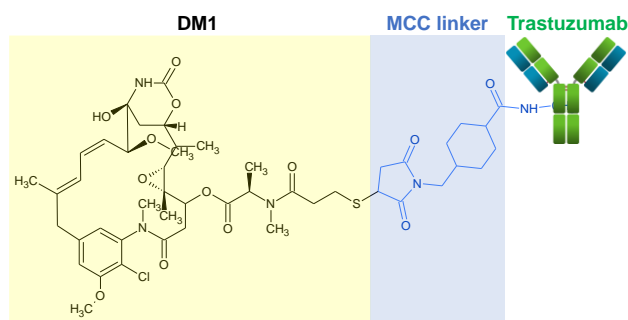


Figure 2. Structure of the T-DM1 ADC. T-DM1 consists of the cytotoxin DM1 (in yellow background) conjugated to trastuzumab via the MCC linker (in blue background), which is covalently bound to the primary amines on the mAb.

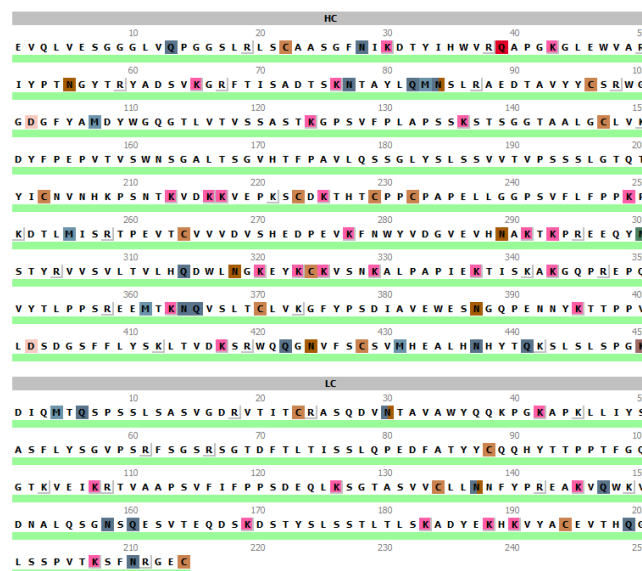


Figure 3. Complete sequence coverage of the LC and HC subunits of trastuzumab from T-DM1. EAD-based peptide mapping led to 100% sequence coverage of LC and HC of trastuzumab in a single injection.

provide 100% sequence coverages of the light chain (LC) and heavy chain (HC) subunits of trastuzumab from T-DM1 in a single injection (Figure 3). This result allowed confident sequence confirmation of trastuzumab and in-depth characterization of DM1-containing peptides.

Characterization of DM1-containing peptides

The unique ability of EAD to retain intact labile modifications in the fragments was leveraged here to provide accurate localization of the payload in DM1-containing peptides.

Figure 4 shows the deisotoped EAD spectrum of the DM1-containing HC peptide (HC222-251) from trastuzumab. EAD led to the generation of extensive *c/y/z* fragments with or without DM1, enabling the confident identification of the peptide sequence and precise localization of the payload. Specifically, the detection of an unmodified c_3 and DM1-containing c_4 fragments pinpointed the position of DM1 to the Lys²²⁵ residue among 3 potential conjugation sites (Lys²²⁵, Lys²⁴⁹ and Lys²⁵¹) in the peptide HC222-251. The Lys²⁴⁹ residue was also identified as a DM1 conjugation site from EAD of the peptide HC229-232 (data not shown). In addition to generating dominant sequence-related fragments, EAD of HC222-251 produced a diagnostic fragment of DM1 at *m/z* 547.2 (Figure 4), facilitating the confirmation of the payload structure.

Figure 5 displays the EAD spectra of the peptide LC25-45 with or without the DM1 payload. EAD provided excellent fragmentation

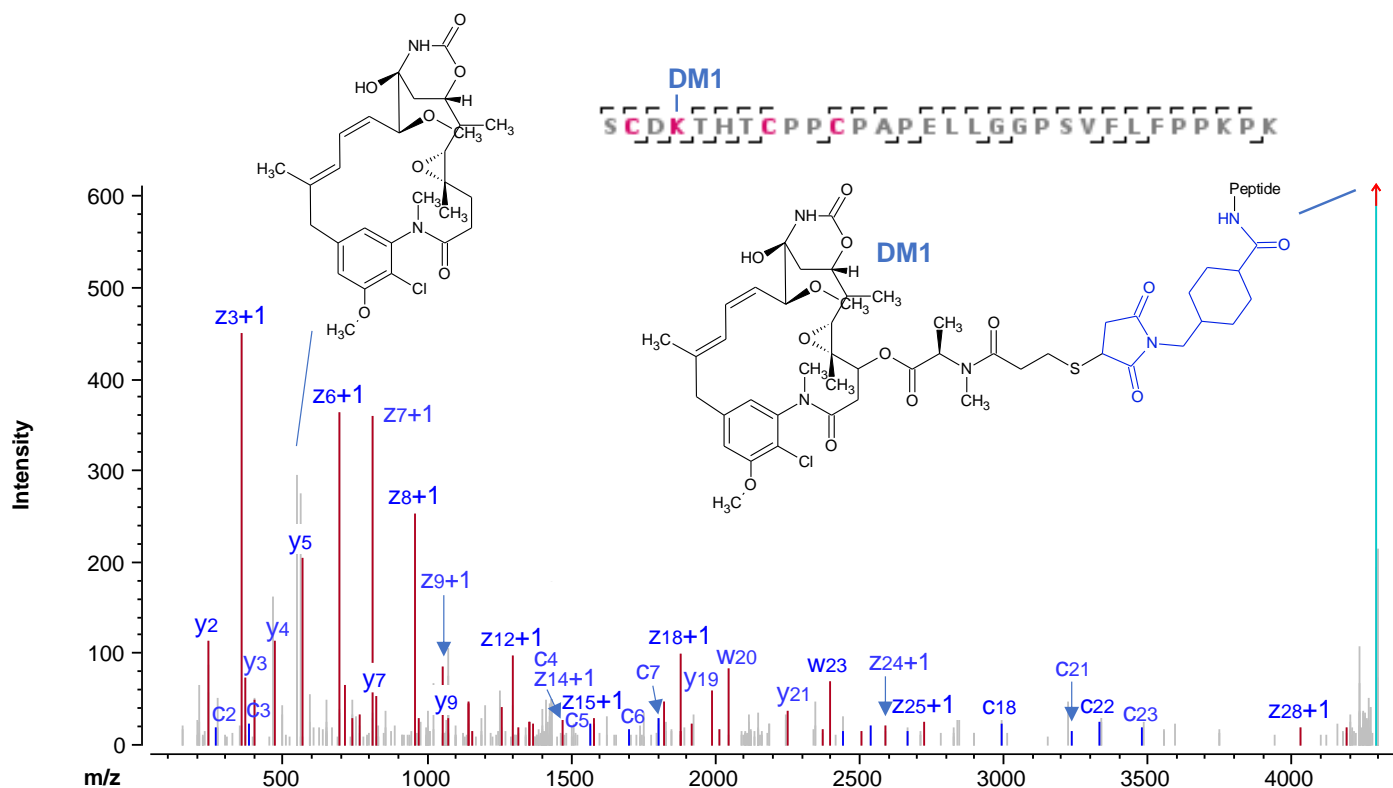


Figure 4. Deisotoped EAD spectrum of the DM1-containing peptide HC222-251 (4+) from Biologics Explorer software. The detection of rich *c/y/z* fragments allowed the accurate localization of DM1 to the Lys²²⁵ residue in this peptide. The peak at *m/z* 547.2 corresponds to a characteristic fragment from the DM1 payload.

of 2 peptides for confident sequence confirmation. Similar to the peptide HC222-251 described above, the sequence of LC25-45 contains 3 potential sites of DM1 conjugation (Lys³⁹, Lys⁴² and Lys⁴⁵). The detection of the fragment at *m/z* 547.2 indicated the presence of the DM1 payload in this LC peptide. The Lys⁴² residue was determined to be the DM1 conjugation site in this LC peptide based on the detection of the unmodified *z*₃+1 and DM1-containing *z*₄+1 ions (Figure 5B).

The streamlined, EAD-based peptide mapping workflow is a powerful tool for comprehensive ADC characterization in a single injection. The unique capabilities of EAD offered by the ZenoTOF 7600 system coupled with automated data interpretation using Biologics Explorer software enabled simultaneous sequence confirmation and payload localization for ADCs with high confidence.

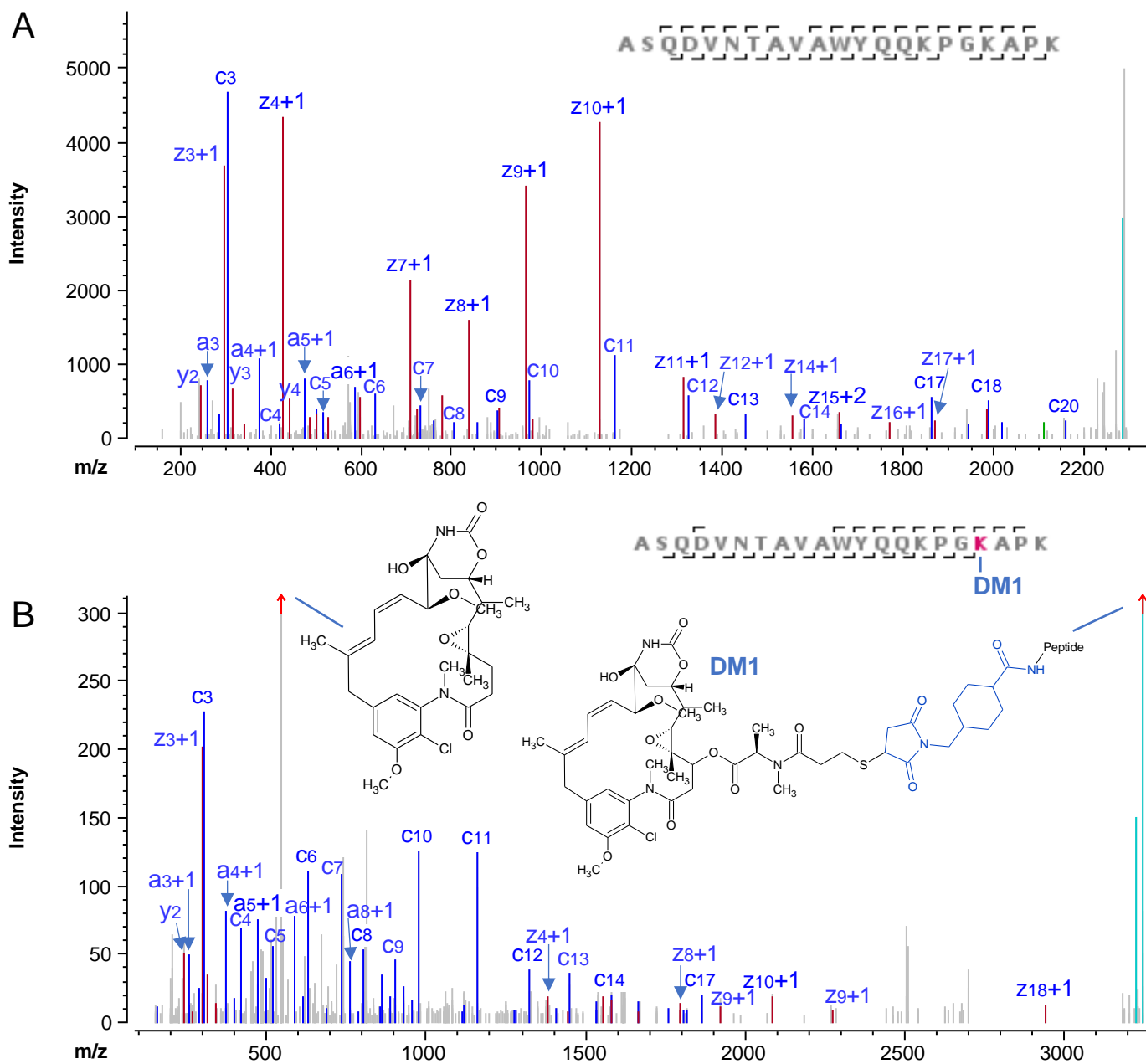


Figure 5. Deisotoped EAD spectra of the peptide LC25-45 (4+) with or without the DM1 from Biologics Explorer software. EAD led to a nearly complete fragment coverage of the peptide LC25-45 (A) without or (B) with the DM1 payload. The peak at m/z 547.2 in B corresponds to a characteristic fragment from the DM1 payload.

Conclusions

- The EAD-based peptide mapping workflow enables comprehensive characterization of complex ADCs in a single injection
- EAD DDA provided a complete sequence coverage of the LC and HC subunits of trastuzumab from T-DM1
- EAD led to extensive fragmentation of DM1-containing peptides for their confident identification while preserving the intact payload for its accurate localization
- EAD DDA coupled with automated data interpretation using Biologics Explorer software offers a streamlined process for biotherapeutic characterization
- The EAD-based peptide mapping workflow requires minimal method development and is easy to implement by different levels of users

References

1. Takashi Baba *et al.* (2015) Electron capture dissociation in a branched radio-frequency ion trap. [Anal Chem, 87\(1\), 785-792.](#)
2. Takashi Baba *et al.* (2021) Dissociation of Biomolecules by an Intense Low-Energy Electron Beam in a High Sensitivity Time-of-Flight Mass Spectrometer. [J Am Soc Mass Spectrom. 32\(8\):1964-1975.](#)
3. An evaluation of a single injection platform method for advanced characterization of protein therapeutics using electron activation dissociation (EAD). [SCIEX technical note, RUO-MKT-02-13965-A.](#)
4. Aliain Beck *et al.* (2010) Strategies and challenges for the next generation of therapeutic antibodies. [Nat Rev Immunol 10\(5\):345-52.](#)
5. Thomas Botzanowski *et al.* (2017) Insights from native mass spectrometry approaches for top- and middle- level characterization of site-specific antibody-drug conjugates. [Mabs, 9\(5\):801-811.](#)
6. Liuxi Chen *et al.* (2016) In-depth structural characterization of Kadcyla (ado-trastuzumab emtansine) and its biosimilar candidate. [Mabs, 8\(7\): 1210-1223.](#)

The SCIEX clinical diagnostic portfolio is For In Vitro Diagnostic Use. Rx Only. Product(s) not available in all countries. For information on availability, please contact your local sales representative or refer to www.sciex.com/diagnostics. All other products are For Research Use Only. Not for use in Diagnostic Procedures.

Trademarks and/or registered trademarks mentioned herein, including associated logos, are the property of AB Sciex Pte. Ltd. or their respective owners in the United States and/or certain other countries (see www.sciex.com/trademarks).

© 2023 DH Tech. Dev. Pte. Ltd. MKT-28847-A



Headquarters
500 Old Connecticut Path | Framingham, MA 01701 USA
Phone 508-383-7700
sciex.com

International Sales
For our office locations please call the division headquarters or refer to our website at sciex.com/offices

A single-injection workflow for enhanced peptide mapping using collision-induced dissociation (CID) and electron-activated dissociation (EAD)

Featuring the single-injection CID/EAD data-dependent acquisition (DDA) workflow using the ZenoTOF 7600 system and Biologics Explorer software from SCIEX

Haichuan Liu, Elliott Jones and Zoe Zhang
SCIEX, USA

This technical note describes a single-injection CID/EAD DDA workflow for a comprehensive characterization of protein therapeutics with high sensitivity. This workflow combines the advantages of CID and EAD in a single acquisition method with minimal compromise. Compared to the existing CID-based high-resolution mass spectrometry (HRMS) platform methods, there is minimal effect on acquisition rate and sensitivity. The CID/EAD DDA workflow provides high sequence coverage of biotherapeutics (>96%). The addition of EAD fragmentation provides a significant enhancement for the confident identification of short and long peptides, clear differentiation of amino acid isomers and accurate localization of labile post-translational modifications (PTMs), such as N- and O-linked glycosylation.

Peptide mapping is widely used for sequence confirmation and PTM identification for antibody-based therapeutics.¹ Peptide mapping is typically performed with collision-based MS/MS fragmentation methods, such as CID. While CID offers high sensitivity and efficient fragmentation of common peptides, it has limitations in fragmenting long peptides, localizing labile PTMs and differentiating amino acid isomers. By comparison, EAD offers excellent fragmentation of long peptides, accurate localization of labile PTMs and confident isomer differentiation.²⁻⁵

In this work, a single-injection CID/EAD DDA workflow (Figure 1) was developed to provide enhanced peptide mapping of biotherapeutics.

Key features of the single-injection CID/EAD DDA workflow for peptide mapping

- **Single-injection platform method:** The CID/EAD DDA workflow provides high sequence coverage of protein therapeutics in a single injection
- **Easy to implement:** The workflow involves an easy addition of powerful EAD capabilities while maintaining the advantages of the traditional CID technique
- **Confident identification of a wide range of peptides:** CID and EAD provide excellent fragmentation and confident identification of short and long peptides, respectively
- **Differentiation of amino acid isomers:** EAD generates diagnostic fragments for clear isomer differentiation
- **Accurate localization of PTMs:** EAD preserves labile PTMs, providing site-specific information about these modifications
- **Powerful software tools:** Biologics Explorer software offers optimized workflow templates and powerful visualization tools for analyzing CID and EAD DDA data in the same file

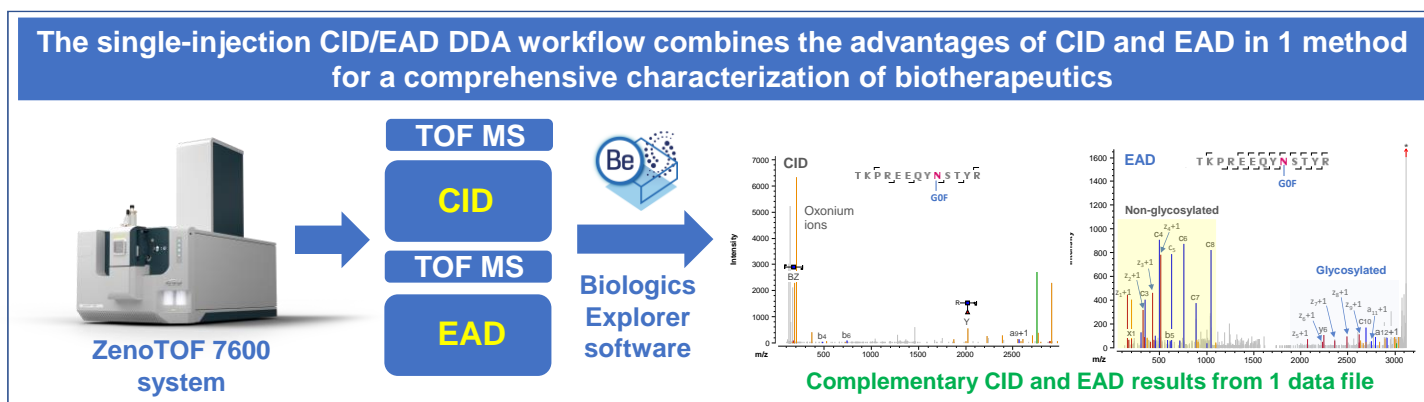


Figure 1. The single-injection CID/EAD DDA workflow combines the advantages of complementary CID and EAD techniques in 1 DDA method. This powerful workflow leverages the fast scanning rate provided by the ZenoTOF 7600 system and streamlined data analysis using Biologics Explorer software. The workflow offers high sequence coverage, confident identification of short and long peptides, clear differentiation of amino acid isomers and accurate localization of labile PTMs while requiring minimal adjustment to the existing CID platform method.

Methods

Sample preparation: NISTmAb (RM8671, NIST) and etanercept were denatured by guanidine hydrochloride, reduced with dithiothreitol and alkylated using iodoacetamide. The sample solution was buffer-exchanged into 50mM Tris-HCl (pH = 7.4) using Bio-Spin columns (Bio-Rad), followed by enzymatic digestion at 37°C for 2-4 h using trypsin/LysC (Promega). The etanercept digest was further incubated with SialEXO (Genovis) at 37°C for 4 h to remove sialic acids. A total of 5–10 µL of the final solution (~5–10 µg) was injected for LC-MS analysis.

Chromatography: The peptides were separated with an LC gradient, displayed in Table 1, using a Waters ACQUITY CSH C18 column (2.1 × 150 mm, 1.7 µm, 130 Å). A flow rate of 0.25 mL/min was used for the separation. The column was kept at 60°C in the column oven of an ExionLC AD system from SCIEX. The mobile phases A and B consisted of 0.1% formic acid (FA) in water and 0.1% FA in acetonitrile, respectively.

Table 1. LC gradient for peptide separation.

Time (min)	A (%)	B (%)
Initial	98	2
2	98	2
62	65	35
65	50	50
67	10	90
70	90	10
71	98	2
75	2	98

Mass spectrometry: DDA experiments were performed in SCIEX OS software using the ZenoTOF 7600 system. The CID/EAD DDA method was created by adding an EAD DDA event to the existing CID platform method. The key TOF MS and DDA settings are listed in Tables 2 and 3, respectively.

Data processing: CID/EAD DDA data were analyzed using an optimized peptide mapping workflow template in Biologics Explorer software. The fragment ions considered for peptide mapping included the primary fragments from the peptide backbone cleavage, such as *a/b/c* and *x/y/z*, and diagnostic fragments for isomer differentiation, such as *c+57/z-57* ions for the differentiation of aspartic acid (Asp) vs. isoaspartic acid (isoAsp) and *w* ions for the differentiation of leucine (Leu) vs. isoleucine (Ile). While N-linked glycosylation was considered for NISTmAb, both N- and O-linked glycosylations were searched when analyzing etanercept DDA data.

Table 2. TOF MS parameters.

Parameter	Value
Spray voltage	5500 V
TOF start mass	400 m/z
TOF stop mass	1800 m/z
Accumulation time	0.08 s
Source temperature	400°C
Declustering potential	80 V
Collision energy	10 V
Time bins to sum	8

Table 3. DDA parameters using CID or EAD.

Parameter	CID	EAD
Start mass	100 m/z	100 m/z
Stop mass	2000 m/z	3000 m/z
Q1 resolution	Unit	Unit
Zeno trap	ON	ON
Zeno threshold	100,000 cps	100,000 cps
Maximum candidate ions	8	6
Charge state	1-5	2-10
Accumulation time	0.05 s	0.08 s
Declustering potential	80 V	80 V
CE	Dynamic	10 V
Time bins to sum	8	8
Electron beam current	N/A	5500 nA
Electron KE	N/A	7 eV
ETC	N/A	Dynamic
Reaction time	N/A	20 ms
EAD RF	N/A	120 Da

High sequence coverage obtained using the CID/EAD DDA workflow

The success of the single-injection CID/EAD DDA workflow was built upon the fast scanning rate of the ZenoTOF 7600 system and the enhanced MS/MS sensitivity offered by the Zeno trap, which increases the detection of MS/MS fragments by 5- to 10-fold.⁶ Traditional electron-based MS/MS (ExD) approaches suffer from low sensitivity and long reaction times. As a result, these ExD approaches are not suitable for routine peptide mapping as a platform method. By comparison, Zeno EAD benefits from high sensitivity, short reaction times (10-20 ms) and fast scanning rates (up to 20 Hz in DDA mode).²⁻⁶ These advantages allowed the implementation of EAD DDA as a platform method for peptide mapping² or a powerful addition to the existing CID platform method to achieve a complete characterization of biotherapeutics. The CID/EAD DDA method combines the strengths of CID in sensitivity and fragmentation of singly charged peptides with the unique capabilities of EAD for fragmentation of long peptides, isomer differentiation and PTM analysis.

Combining complementary CID and EAD techniques in the same DDA method led to consistently high sequence coverage. Figure 2 shows that the CID/EAD DDA method provided a nearly complete sequence coverage (>96%) of NISTmAb light chain (LC) and heavy chain (HC) from 1 trypsin/LysC digest in a single injection. This result is comparable to or slightly better than that obtained using CID or EAD DDA alone (data not shown).

Confident identification of short and long peptides

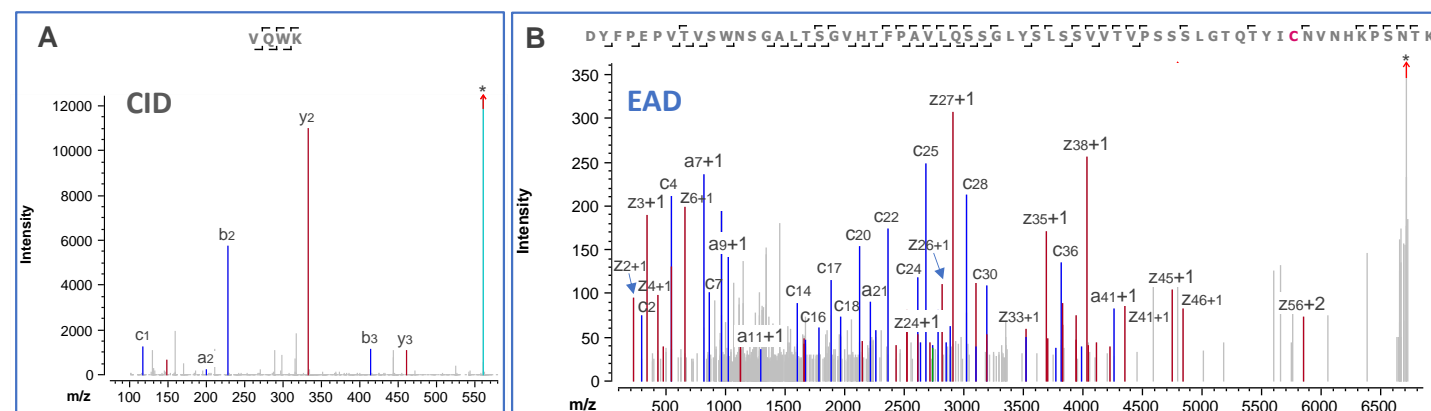


Figure 3. Confident identification of short peptides using CID and long peptides using EAD. The CID/EAD DDA workflow allowed excellent fragmentation and confident identification of a singly charged peptide VQWK from NISTmAb LC by CID (A) and a multiply charged long peptide (~6.7 kDa) from NISTmAb HC by EAD (B). Not all fragments in the spectra are labeled for spectral clarity. All the MS/MS spectra in this technical note are the deisotoped spectra taken directly from Biologics Explorer software. The peaks labeled with * are the deisotoped precursors.

HC, 96.9%



LC, 99.1%

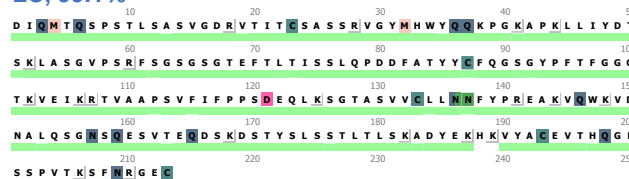


Figure 2. The single-injection CID/EAD DDA workflow offers high sequence coverage (>96%) of NISTmAb LC and HC from 1 trypsin/LysC digest. The CID/EAD workflow provided comparable or slightly better sequence coverages of 2 NISTmAb chains than the CID or EAD method alone.

Depending on the frequency of the Arg and Lys residues in the sequence, trypsin digestion of protein therapeutics might lead to short peptides containing ≤ 5 amino acid residues or long peptides larger than >5 kDa. CID and EAD have different strengths in the fragmentation of short vs. long peptides. While CID offers excellent fragmentation of short peptides in low charge states (1+ or 2+), EAD is superior for the characterization of multiply charged long peptides ($\geq 3+$). The CID/EAD DDA

workflow provides the combined advantages of these 2 techniques to cover a full spectrum of peptides with various sizes or charge states.

Figure 3 shows the CID spectrum of a singly charged peptide VQWK and the EAD spectrum of a long tryptic peptide (~6.7 kDa). Excellent fragmentation of these 2 peptides using CID or EAD led to their confident identification in 1 experiment. The ability of the CID/EAD DDA method to confidently identify short and long peptides enables consistently high sequence coverage of protein therapeutics from single enzymatic digestion.

Differentiation of amino acid isomers

It is challenging to differentiate amino acid isomers, such as Leu vs. Ile or Asp vs. isoAsp, using CID MS/MS. By comparison, EAD produces diagnostic fragments to enable a clear differentiation between these amino acid isomers.^{2,4} Therefore, including EAD in the CID/EAD DDA method significantly enriches the information for peptide mapping to achieve a complete characterization of biotherapeutics in a single injection.

Figure 4 shows the zoomed-in views of signature fragments for the confirmation of Leu and Ile residues in the peptide ALPAPIEK from the NISTmAb HC. The detection of z_{7+1-43} and z_{3+1-29} fragments confirmed the presence of 2 amino acid residues in their respective positions in this peptide.

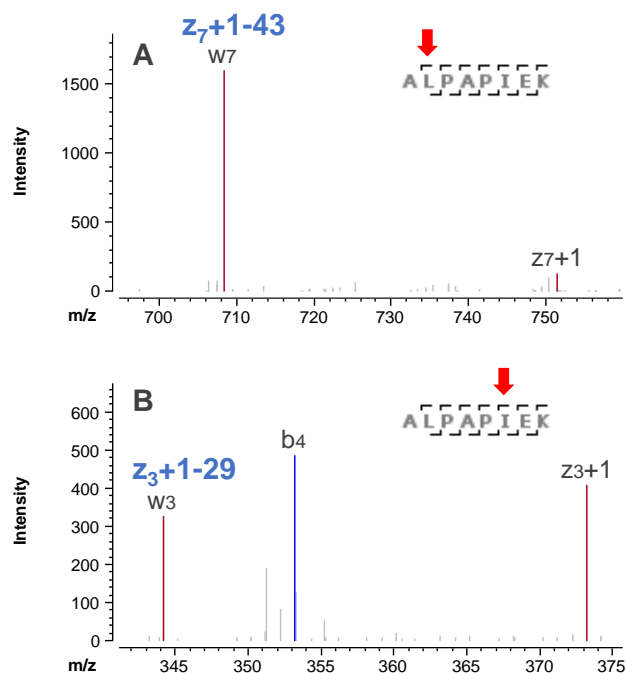


Figure 4. Confirmation of Leu vs. Ile residues using diagnostic EAD fragments. The Leu² and Ile⁶ residues in the peptide ALPAPIEK can be confirmed based on the detection of the signature w_7 or z_{7+1-43} ion for Leu (A) and the w_3 or z_{3+1-29} ion for Ile (B), respectively, in the EAD DDA data.

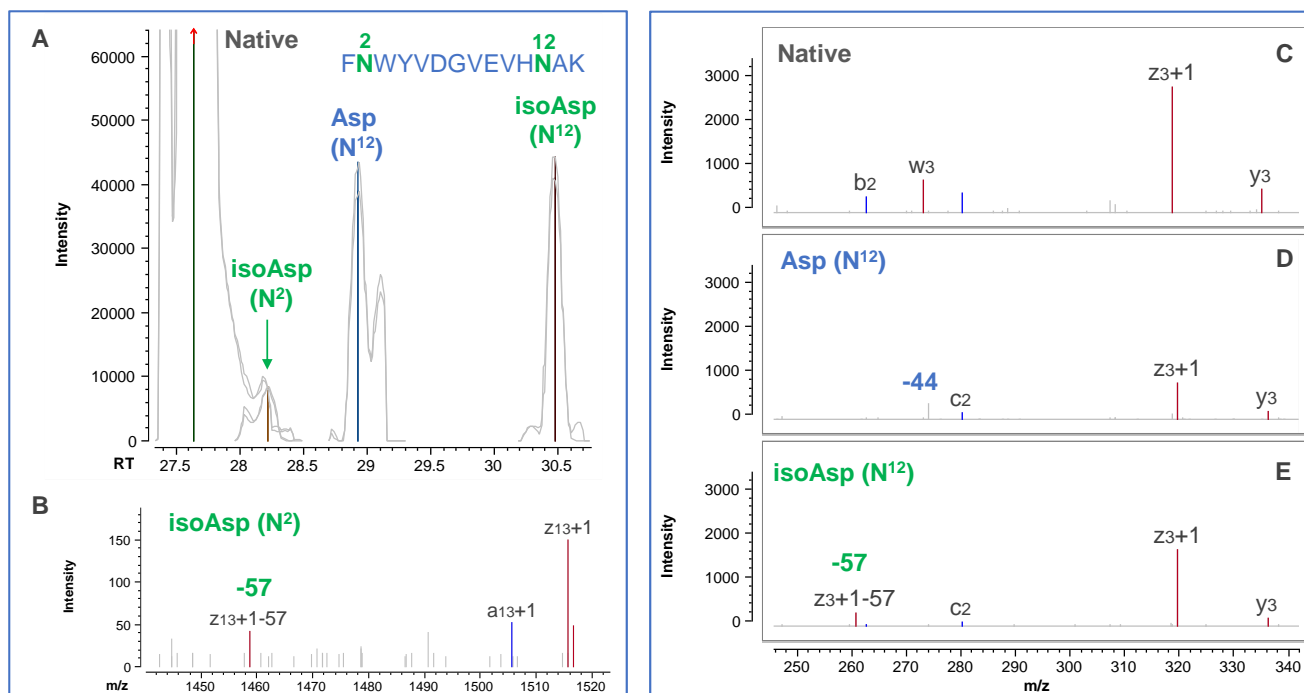


Figure 5. Identification and differentiation of Asp vs. isoAsp isomers using EAD. Three deamidation isomers were identified in the extracted ion chromatogram (XIC) of the peptide FNWYVDGYEVHNAK (A). EAD led to the differentiation of these 3 isomers based on the detection of z_{-57} or z_{-44} fragments (B-E). The detection of a $z_{13+1-57}$ ion (B) confirmed the isoAsp isomer from N² deamidation (B), while the detection of a z_{3+1-44} or z_{3+1-57} fragment enabled the differentiation of Asp vs. isoAsp isomers from N¹² deamidation (D and E).

Figure 5 shows an example of using EAD to identify and differentiate 3 deamidation isomers of the peptide FNWYVDGYEVHNAK from the NISTmAb HC. The 3 isomers identified in the XIC (Figure 5A) were produced from the deamidations of the Asn² (N²) or Asn¹² (N¹²) residue in this peptide. The detection of a z₁₃+1-57 fragment in EAD of the N²-deamidated species led to the confident assignment of this species as the isoAsp isomer (Figure 5B). Similarly, the N¹²-deamidated species eluting at ~30 min was an isoAsp isomer based on the detection of a z₃+1-57 ion (Figure 5E). The absence of this diagnostic fragment and the detection of a z₃+1-44 ion for the N¹²-deamidated species eluting at ~29 min confirms that this species was an Asp isomer (Figure 5D).

Comprehensive characterization of glycosylation

The CID/EAD DDA workflow combines the complementary capabilities of CID and EAD for the comprehensive characterization of glycopeptides. While CID preferentially cleaves the glycan to produce diagnostic oxonium ions, EAD preserves this labile modification for its confident identification and accurate localization.

Figure 6 shows the CID and EAD spectra of an N-linked glycopeptide TKPREEQYNSTYR carrying a G0F moiety. The detection of abundant oxonium ions, such as m/z 204 Da, in the CID spectrum (Figure 6A) confirms the presence of glycosylation in this peptide. However, CID led to insufficient sequence coverage and a lack of information about the site of glycosylation. By comparison, EAD produced a nearly complete series of sequence fragments with or without glycosylation, enabling the accurate localization of the G0F glycan.

Figure 7 highlights the power of EAD for the characterization of 2 O-linked glycopeptides in etanercept.³ EAD provided extensive fragmentation of these 2 glycopeptides while preserving the labile O-glycan in the fragments, enabling confident peptide

Table 4. The CID/EAD workflow provides a comprehensive characterization of protein therapeutics.

Characterizations	
High sequence coverage	✓
Singly charged short peptides	✓
Long peptides (>5 kDa)	✓
Isomer differentiation	✓
Localization of labile PTMs	✓
Disulfide bond mapping	✓

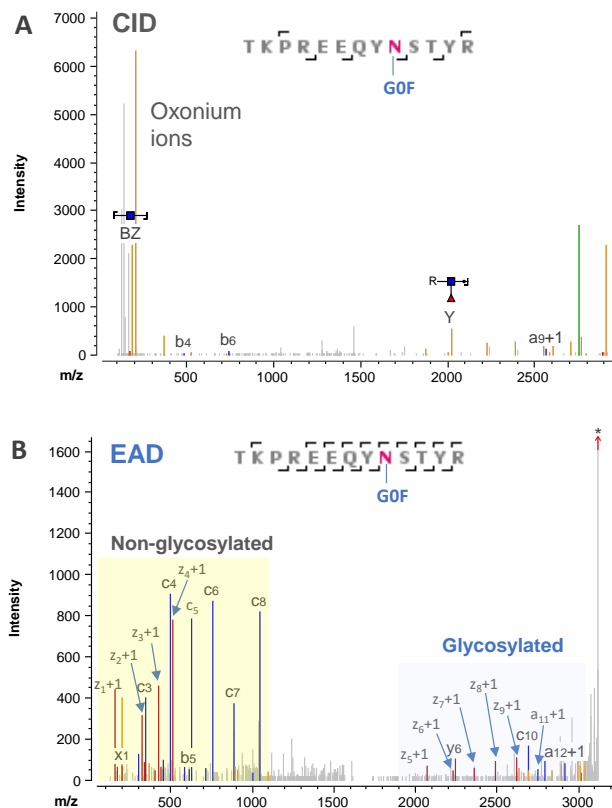


Figure 6. Characterization of N-linked glycosylation in NISTmAb using CID and EAD. The CID/EAD workflow provided complementary DDA data for confident identification and localization of N-linked glycosylation. While CID generated abundant oxonium ions to confirm the presence of glycosylation in the peptide TKPREEQYNSTYR (A). EAD provided a nearly complete series of c/z ions with (in blue background) or without (in yellow background) glycosylation (B). Specifically, the detection of non-glycosylated z₁-z₄ and glycosylated z₅-z₉ fragments allowed the accurate localization of the G0F glycan to the Asn residue. The peak labeled with * in B is the deisotoped precursor.

identification and glycosylation site determination. Specifically, the O-glycan site in the peptide THTCPPCAPELLGGPSVFLFPPKPK was pinpointed to the Thr³ residue, which is 1 of 3 potential O-glycosylation sites in this peptide, based on the detection of non-glycosylated c₂ and glycosylated c₃ fragments (Figure 7A). Similarly, the 2 O-glycans in the peptide SMAPGAVHLPQPVSTR were confidently localized to the Ser and Thr residues near the C-terminus based on the glycosylation status of z₁-z₃ fragments (Figure 7B).

In summary, the CID/EAD DDA workflow provides the combined benefits of 2 complementary MS/MS techniques, as summarized in Table 4, to achieve a complete characterization of protein therapeutics. The workflow offers high sequence coverage, confident identification of short and long peptides, clear differentiation of amino acid isomers and accurate localization of

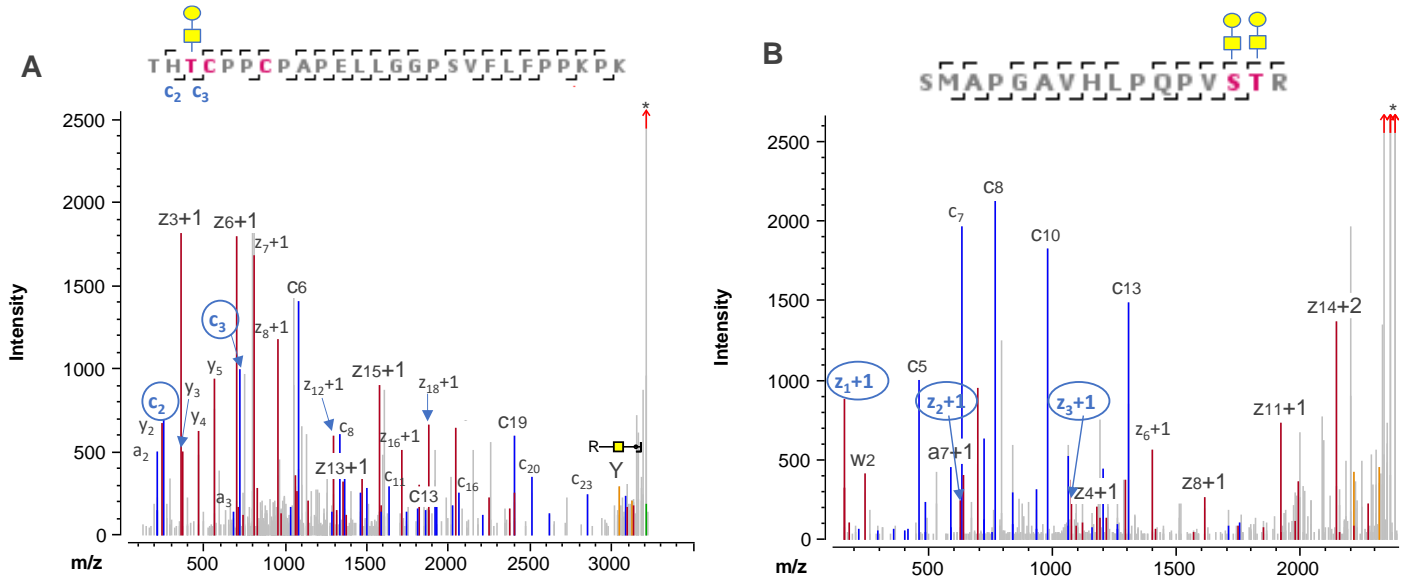


Figure 7. Accurate localization of O-linked glycosylation in etanercept using EAD. The location of 1 HexHexNAc moiety in the glycopeptide THTCPPCPAPELLGGPSVFLFPPKPK was pinpointed to the Thr³ residue, out of 3 potential O-linked glycosylation sites including 2 Thr and 1 Ser, based on the detection of non-glycosylated c₂ and glycosylated c₃ fragments (circled in A). Similarly, the sites of 2 O-glycans in the glycopeptide SMAPGAVHLPQPVSTR were confidently determined based on the detection of z₁-z₃ (circled in B) with 0, 1 and 2 HexHexNAc moieties, respectively. The peaks labeled with * are the deisotoped precursors.

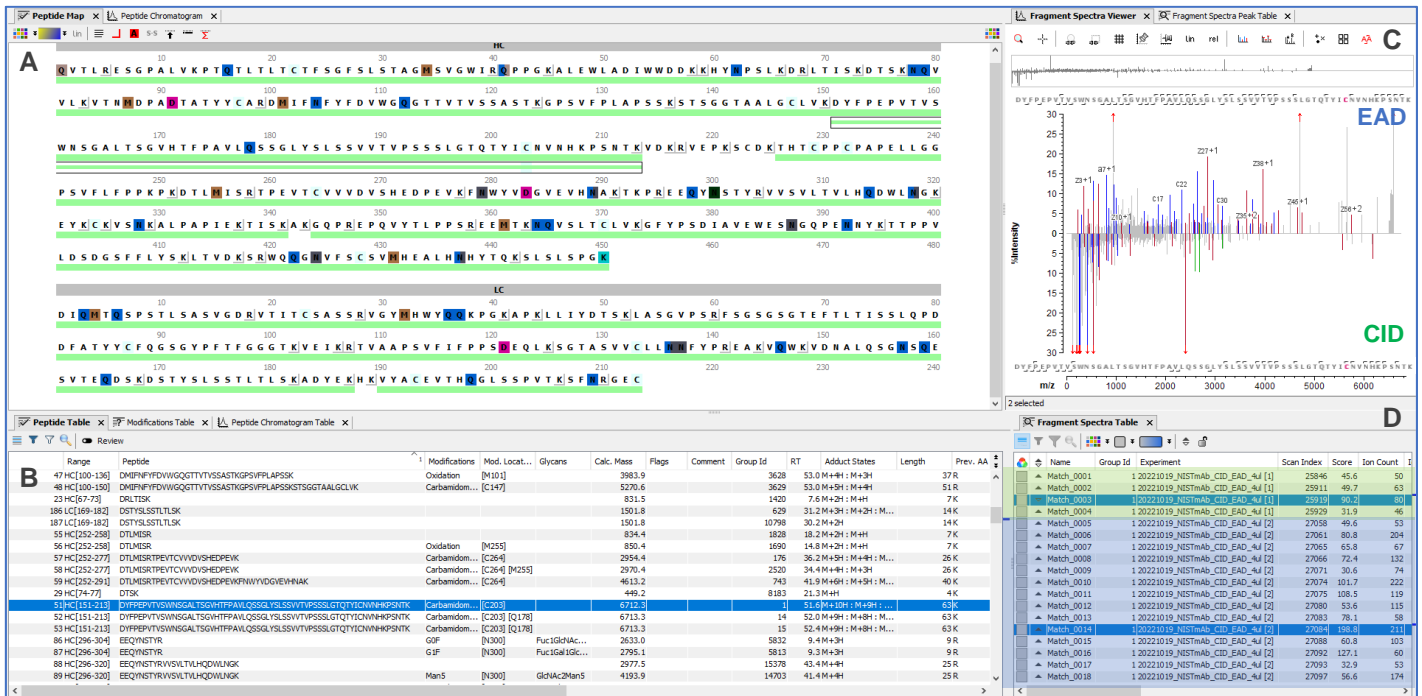


Figure 8. Biologics Explorer software provides user-friendly interfaces for reviewing and comparing the CID/EAD DDA results. Biologics Explorer software offers a streamlined and automatic workflow template for processing the CID and EAD data in the same raw file. The software provides the combined sequence coverage (A) based on the identified peptides, which are listed in the peptide table (B). The fragment spectra viewer (C) displays the individual or combined CID or EAD spectra with annotations, depending on the spectral selection in the fragment spectra table (D). The spectra can be visualized or compared using different tools such as a stacked view or mirror plot (C). The fragment spectra table compiles all the annotated CID and EAD spectra, as highlighted in the green and blue backgrounds, respectively (D). The peptide highlighted in this figure is the long peptide described in the previous section (Figure 3B). It is evident from the annotated spectra (C) that EAD provided more extensive fragmentation and a higher sequence coverage of this long peptide compared to CID.

labile PTMs while requiring minimal adjustment to the existing CID platform method (Table 4). The advantage of the CID/EAD workflow for disulfide bond mapping will be highlighted in a future technical note.

Powerful software tools for data processing and results review

Biologics Explorer software offers streamlined peptide mapping templates optimized for DDA data from the ZenoTOF 7600 system. In addition, the software provides an array of effective tools to facilitate results review and comparison for improved user experience.

Figure 8 shows the default view of the peptide mapping result from the CID/EAD DDA analysis of NISTmAb. The peptide map tab (Figure 8A) provides a quick overview of the sequence coverage of the HC and LC. The peptide table (Figure 8B) lists all peptides identified using CID and/or EAD. The annotated MS/MS spectra of the highlighted peptide in the peptide table can be visualized and compared in the fragment spectra viewer (Figure 8C), depending on the spectral selection in the fragment spectra table (Figure 8D).

Conclusions

- The single-injection CID/EAD DDA workflow combines the advantages of complementary CID and EAD techniques and offers a comprehensive characterization of biotherapeutics
- This powerful workflow maintains the capabilities of the traditional CID DDA platform method while offering additional benefits from EAD in the same data file
- The CID/EAD DDA workflow led to high sequence coverage (>96%) of LC and HC from 1 trypsin digest of NISTmAb in a single injection
- The workflow couples the ultrahigh sensitivity and confident identification of short peptides offered by CID with excellent fragmentation and improved confidence in the characterization of long peptides using EAD
- EAD enabled confident differentiation of amino acid isomers, such as Leu vs. Ile and Asp vs. isoAsp, and accurate localization of N- and O-linked glycosylation

- Biologics Explorer software provides optimized peptide mapping workflow templates and powerful visualization tools for streamlined data processing and improved user experience with results review and comparison

References

1. Anna Robotham and John Kelly. (2020) LC-MS characterization of antibody-based therapeutics: recent highlights and future prospects. [Approaches to the Purification, Analysis and Characterization of Antibody-Based Therapeutics. Chapter 1:1-33.](#)
2. An evaluation of a single injection platform method for advanced characterization of protein therapeutics using electron activation dissociation (EAD). [SCIEX technical note, RUO-MKT-02-13965-A.](#)
3. Comprehensive characterization of O-linked glycosylation in etanercept by electron activated dissociation (EAD). [SCIEX technical note, RUO-MKT-02-14921-A.](#)
4. Comprehensive differentiation of deamidation isomers from forced degradation by electron activation dissociation (EAD). [SCIEX technical note, RUO-MKT-02-14730-A.](#)
5. Monitoring and determining the cause of antibody discoloration using capillary isoelectric focusing (cIEF) and electron activated dissociation (EAD). [SCIEX technical note, MKT-26819-A.](#)
6. Takashi Baba *et al.* (2021) Dissociation of biomolecules by an intense low-energy electron beam in a high sensitivity time-of-flight mass spectrometer. [J. Am. Soc. Mass Spectrom. 32\(8\):1964-1975.](#)

The SCIEX clinical diagnostic portfolio is For In Vitro Diagnostic Use. Rx Only. Product(s) not available in all countries. For information on availability, please contact your local sales representative or refer to www.sciex.com/diagnostics. All other products are For Research Use Only. Not for use in Diagnostic Procedures.

Trademarks and/or registered trademarks mentioned herein, including associated logos, are the property of AB Sciex Pte. Ltd. or their respective owners in the United States and/or certain other countries (see www.sciex.com/trademarks).

© 2023 DH Tech. Dev. Pte. Ltd. MKT-28039-A



Headquarters
 500 Old Connecticut Path | Framingham, MA 01701 USA
 Phone 508-383-7700
sciex.com

International Sales
 For our office locations please call the division headquarters or refer to our website at sciex.com/offices

A streamlined workflow for the determination of the drug-to-antibody ratio (DAR) of antibody-drug conjugates (ADCs)

Featuring the intact protein analysis workflow using the ZenoTOF 7600 system and Biologics Explorer software from SCIEX

Rashmi Madda, Haichuan Liu and Zoe Zhang
SCIEX, USA

This technical note highlights an efficient intact protein analysis workflow for determining drug-to-antibody ratios (DARs) of antibody-drug conjugates (ADCs)¹. This workflow leverages high-resolution mass spectrometry (MS) for accurate intact mass measurement in addition to automated protein deconvolution and DAR calculation provided by Biologics Explorer software. Average DAR values of 3.6 and 3.5 were obtained for the glycosylated (native) and deglycosylated forms of trastuzumab emtansine (T-DM1), respectively.

ADCs—a new generation of biotherapeutics—combine potent cytotoxic drugs with monoclonal antibodies (mAbs) that target specific cells.¹ The drug and mAb are connected through a cysteine-based, lysine-based or site-specific linker. Depending on the type of linkage used in an ADC, DAR values as high as 8 might be observed.² This variability underscores the need for accurate and reliable DAR measurements to optimize ADC performance and efficacy.³ The mean quantity of drugs conjugated to antibodies is a critical parameter for ADCs. Therefore, DAR measurement is pivotal in determining essential properties, such as drug clearance, pharmacokinetics and biodistribution, which are vital considerations for developing targeted therapies.

In this work, the glycosylated and deglycosylated forms of T-DM1 were characterized using the ZenoTOF 7600 system, followed by automated data analysis using Biologics Explorer software (Figure 1), leading to accurate DAR measurements in a streamlined workflow.

Key features of the intact protein analysis workflow for ADC characterization

- **Efficient:** The streamlined workflow leverages high-resolution MS for accurate mass measurement of intact ADCs and powerful software tools for automated DAR calculation
- **Accurate DAR measurement:** Biologics Explorer software offers powerful algorithms for confident protein deconvolution and accurate DAR calculation
- **Easy to implement:** The integrated workflow and intuitive software interface make ADC analysis accessible to various researchers, regardless of their expertise level
- **Routine ADC characterization:** This workflow can be rapidly implemented for routine ADC characterization to ensure product quality

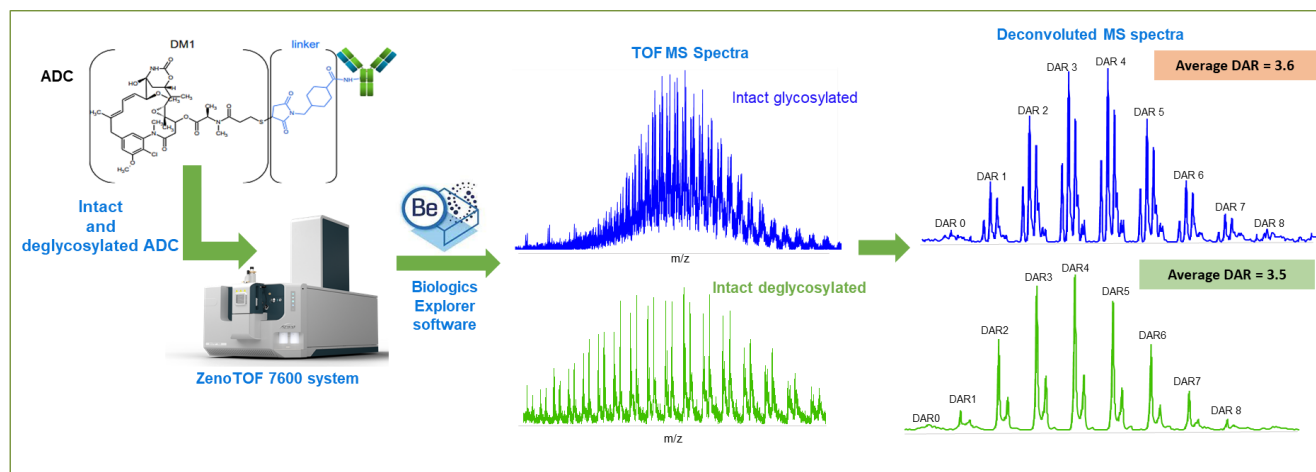


Figure 1. A streamlined intact mass analysis workflow for determining the average DAR values of the glycosylated and deglycosylated forms of T-DM1 using the ZenoTOF 7600 system. Intact T-DM1 MS data were analyzed by Biologics Explorer software using an optimized intact mass analysis workflow template for automated DAR calculation. Average DAR values of 3.6 and 3.5 were obtained for the glycosylated and deglycosylated forms of T-DM1, respectively.

Methods

Sample preparation: Lyophilized T-DM1 was reconstituted in deionized (DI) water to a final concentration of 5 mg/mL. For the intact ADC analysis, the reconstituted T-DM1 was diluted with 0.1% formic acid (FA) in water to 1 mg/mL prior to LC/MS analysis. Deglycosylation of T-DM1 was performed by adding 1 μ L of 50 units/ μ L PNGase F (Sigma-Aldrich) in 20mM Tris-HCl buffer (pH = 8.2) to 100 μ L of 1 μ g/ μ L T-DM1 (100 μ g). The mixture was incubated overnight at 37°C. Finally, 5 μ L samples of T-DM1 were injected for LC-MS analysis.

Chromatography: Intact glycosylated and deglycosylated ADC samples were separated using the LC gradient displayed in Table 1, using a Waters ACQUITY BEH C4 column (2.1 mm x 50 mm, 1.7 μ m, 300 Å, Waters). The flow rate was set to 0.3 mL/min for all LC runs. The column was kept at 60°C in the column oven of an ExionLC AD system (SCIEX). Mobile phases A and B consisted of 0.1 % FA in water and 0.1% FA in acetonitrile, respectively.

Table 1. Chromatographic gradient for T-DM1 separation.

Time (min)	Mobile phase A (%)	Mobile phase B (%)
0.0	90	10
2	90	10
6	10	90
7	10	90
7.10	95	5
10	95	5

Mass spectrometry: Intact LC-MS data of glycosylated and deglycosylated ADCs were acquired using the ZenoTOF 7600 system (SCIEX). The source parameter and TOF MS settings are listed in Tables 2 and 3.

Data processing: Intact T-DM1 LC-MS data were analyzed using the intact protein analysis workflow template in Biologics Explorer software. The DM1 and linker were added to the conjugate table.

Table 2. Source and gas parameters.

Parameter	Value
Polarity	Positive
Ion source gas 1	50 psi
Ion source gas 2	50 psi
Curtain gas	30 psi
Source temperature	400°C
CAD gas	7

Table 3. TOF MS parameters.

Parameter	Value
Spray voltage	5500 V
TOF start mass	900 m/z
TOF stop mass	4000 m/z
Accumulation time	0.25 s
Declustering potential	250 V
Collision energy	10 V
Time bins to sum	80

Intact protein deconvolution and DAR measurement for T-DM1

To determine the DAR of T-DM1, intact mass measurements of the glycosylated and deglycosylated forms of T-DM1 were performed using the ZenoTOF 7600 system. Complex charge state distributions were observed for the 2 forms of T-DM1 in the high-resolution TOF MS spectra (Figure 2A and 2D). The results of intact protein deconvolution from Biologics Explorer software revealed that the complex MS profile of the glycosylated T-DM1 consists of different glycoforms—mainly G0F, G1F and G2F—conjugated with as many as 8 molecules of the payload DM1 (Figure 2B and 2C). By comparison, the removal of N-linked glycosylation led to a simpler MS profile (Figure 2D–F), where the deglycosylated T-DM1 carrying up to 8 DM1 was detected. The 2 forms of T-DM1 were identified with a <10 ppm mass accuracy and were automatically integrated through Biologics Explorer software. Figure 3 shows the DAR distributions of the glycosylated and deglycosylated forms of T-DM1. In both cases, the major T-DM1 species had a DAR value of 2–4 (Figure 3).

The average DARs of the glycosylated and deglycosylated forms of T-DM1 can be calculated from the DAR distributions within Biologics Explorer software. Average DAR values of 3.6 and 3.5 were measured for the glycosylated and deglycosylated forms of T-DM1, respectively. The measured DAR values agree with those reported for T-DM1 in the literature.^{5,6}

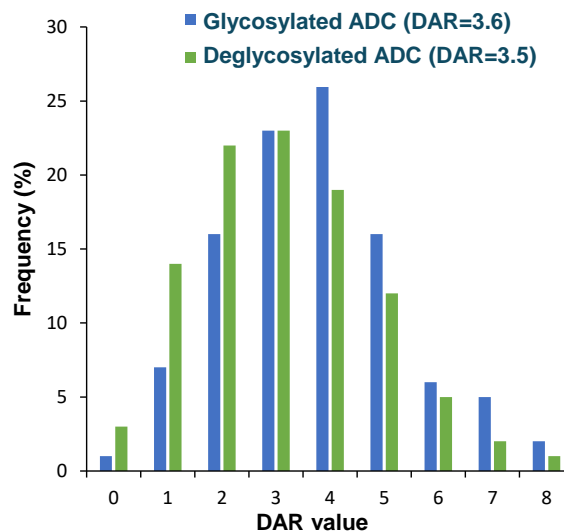


Figure 3. DAR distributions of the glycosylated and deglycosylated forms of T-DM1. Average DAR values of 3.6 and 3.5 were determined for the glycosylated and deglycosylated forms of T-DM1, respectively.

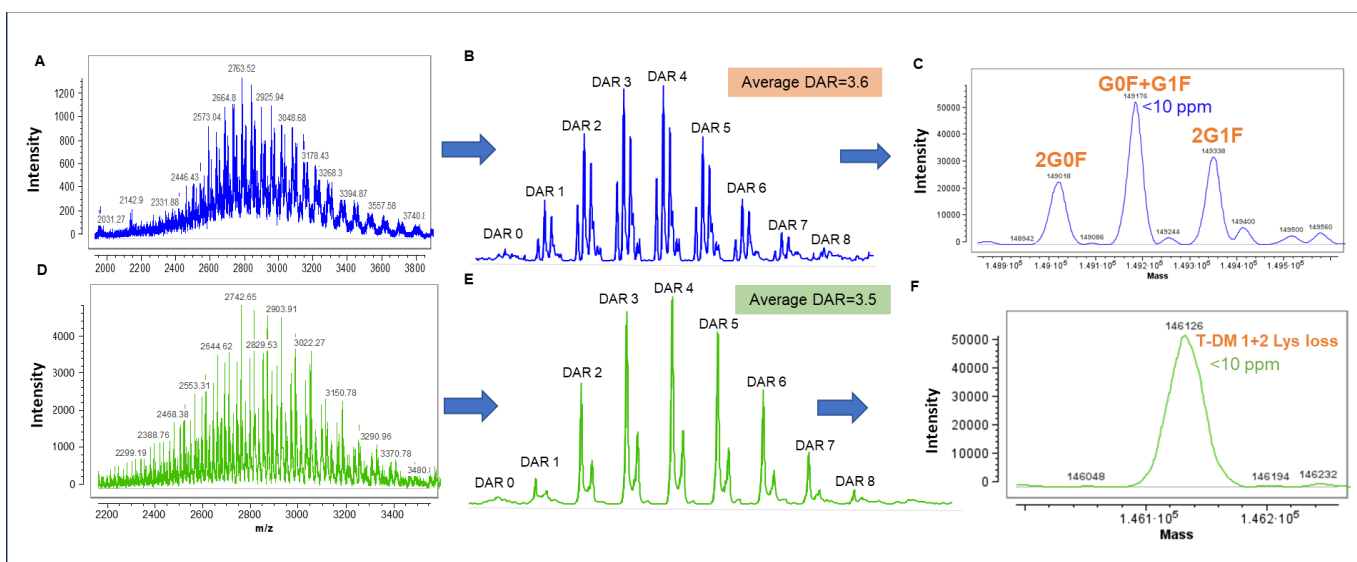


Figure 2. Intact protein deconvolution and DAR measurement of the glycosylated and deglycosylated forms of T-DM1 using Biologics Explorer software. (A and D) Charge state distributions of the glycosylated and deglycosylated forms of T-DM1. (B and E) Deconvoluted mass spectra of the glycosylated and deglycosylated forms of T-DM1 that reveal the DAR distribution of the detected peaks. (C) Zoomed view of the deconvoluted spectrum of the glycosylated form of T-DM1 with 3 major glycoforms annotated. (F) Zoomed view of the deconvoluted spectrum of the deglycosylated form of T-DM1.

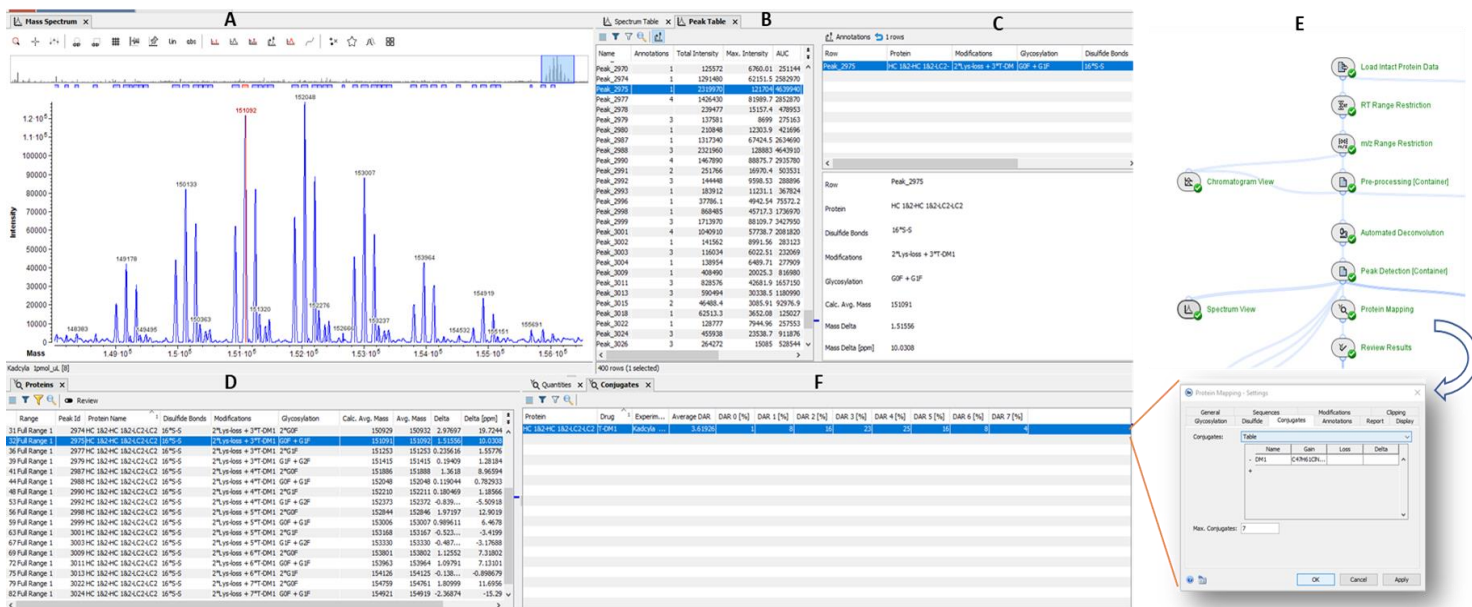


Figure 4. A snapshot of Biologics Explorer software for analyzing T-DM1 data and calculating DAR values. The intact protein analysis workflow within Biologics Explorer software offers streamlined and automated interpretation of intact ADC data. In addition, the software provides powerful tools for reviewing the deconvolution spectrum (A), annotated peaks (B–D) and the results of DAR measurement (F) in the same page. The payload and linker composition can be conveniently defined in the conjugate table within the protein mapping activity of the intact protein analysis workflow (F).

Streamlined ADC analysis using Biologics Explorer software

The analysis of intact ADC data was streamlined in 1 workflow using Biologics Explorer software, as shown in Figure 4. This compelling software displays the deconvoluted spectrum (Figure 4A) and detailed information about the annotated peaks (Figure 4B–D) on a single page for easy results review. Moreover, the payload and linker composition can be conveniently defined in the conjugate table within the protein mapping activity (Figure 4E), which provides an automated average DAR measurement of the glycosylated T-DM1 (Figure 4F). This intuitive template highlights the ability of Biologics Explorer software to seamlessly guide users through accurate measurements and informative data analysis.

Conclusions

- The streamlined, intact protein analysis workflow leverages the power of the ZenoTOF 7600 system for accurate intact mass measurement and automated data interpretation offered by Biologics Explorer software for rapid protein deconvolution and DAR determination
- Accurate mass measurement led to high-confidence annotation of T-DM1 glycoforms conjugated with as many as 8 molecules of the payload
- Average DAR values of 3.6 and 3.5 were measured for the glycosylated and deglycosylated forms of T-DM1, respectively
- Biologics Explorer software provides intuitive workflows and powerful tools for confident protein deconvolution, automated DAR calculation and rapid results review

References

1. Heidi Perez *et al.* (2014) Antibody-drug conjugates current status and future directions. [*Drug Discovery Today* 19\(7\): 869-881.](#)
2. Yutaka Matsuda and Brian Mendelsohn (2021) Recent Advances in Drug-Antibody Ratio Determination of Antibody-Drug Conjugates. [*Chem. Pharm. Bull.* 69\(10\):976-983.](#)
3. Intact Analysis of Antibody Drug Conjugates. [SCIEX technical note, RUO-MKT-02-5468-C.](#)
4. Characterization of an antibody-drug-conjugate (ADC) using electron activated dissociation (EAD). [SCIEX technical note RUO-MKT-02-12834-B.](#)
5. Gail Lewis Phillips *et al.* (2008) Targeting HER2-positive breast cancer with trastuzumab-DM1, an antibody-cytotoxic drug conjugate. [*Cancer Res.* 68\(22\):9280-9290.](#)
6. Rinnerthaler G *et al.* (2019). HER2 Directed Antibody-Drug-Conjugates beyond T-DM1 in Breast Cancer. [*Int J Mol Sci.* 20\(5\):1115.](#)

The SCIEX clinical diagnostic portfolio is For In Vitro Diagnostic Use. Rx Only. Product(s) not available in all countries. For information on availability, please contact your local sales representative or refer to <https://sciex.com/diagnostics>. All other products are For Research Use Only. Not for use in Diagnostic Procedures.

Trademarks and/or registered trademarks mentioned herein, including associated logos, are the property of AB Sciex Pte. Ltd. or their respective owners in the United States and/or certain other countries (see www.sciex.com/trademarks).

© 2023 DH Tech. Dev. Pte. Ltd. MKT-29392-A



Headquarters
500 Old Connecticut Path | Framingham, MA 01701 USA
Phone 508-383-7700
sciex.com

International Sales
For our office locations please call the division
headquarters or refer to our website at
sciex.com/offices

A streamlined single-injection middle-down workflow using electron activated dissociation (EAD) for biotherapeutics characterization

Featuring the ZenoTOF 7600 system and Biologics Explorer software from SCIEX

Haichuan Liu and Zoe Zhang
SCIEX, USA

This technical note highlights the power of a streamlined middle-down workflow using electron activated dissociation (EAD) to achieve high sequence coverages (70%-80%) of monoclonal antibody (mAb) subunits in a single injection. This powerful workflow combines the descriptive and reproducible fragmentation provided by an EAD mechanism with automated data analysis using Biologics Explorer software. As a result, the workflow significantly reduces the time and effort required for middle-down analysis of protein therapeutics.

It is important to confirm the sequences and post-translational modifications (PTMs) of protein therapeutics to ensure drug safety and efficacy.¹ While bottom-up mass spectrometry (MS) provides a complete sequence coverage of protein therapeutics, this technique involves multiple steps of sample preparation, in which modification artifacts are often introduced.² In contrast, top-down MS requires minimal sample preparation. However, it typically results in low sequence coverage of an intact mAb. Middle-down MS combines the advantages of these 2 approaches and offers high sequence coverages of subunits following simple sample preparation.²⁻⁴

Traditionally, a middle-down workflow requires extensive method development and often involves multiple fragmentation techniques and/or injections to obtain high sequence coverage. In addition, commercial software designed for the requirements of biopharmaceutical middle-down data analysis has been lacking in the market. These challenges are addressed by introducing the single-injection EAD-based middle-down workflow (Figure 1), as described in this technical note.

Key features of the EAD-based middle-down workflow

- **High sequence coverage:** 70%-80% sequence coverages were obtained for mAb subunits in a single injection
- **Streamlined:** The workflow consists of simple sample preparation, efficient data acquisition and automatic data analysis
- **Single-injection method:** The EAD-based middle-down workflow can be implemented for routine analysis of mAbs
- **Reproducible:** EAD with the Zeno trap provided reproducible fragmentation and detection of low abundant fragments

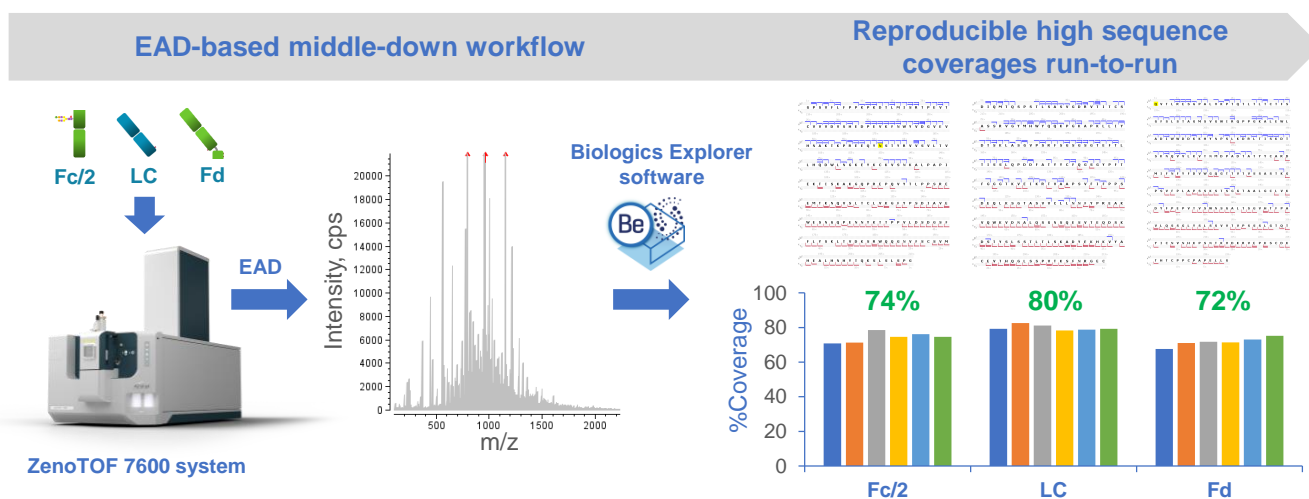


Figure 1. A streamlined EAD-based middle-down workflow for achieving consistently high sequence coverages of mAb subunits from run-to-run. In the EAD-based middle-down workflow, the Fc/2, LC and Fd subunits of mAbs were subjected to EAD fragmentation using the ZenoTOF 7600 system, followed by automatic data processing with a middle-down workflow template in the Biologics Explorer software. This powerful workflow provides consistent high sequence coverages over 6 replicate injections (80% for the LC subunit and 70-75% for the Fc/2 and Fd subunits) while requiring minimal effort for method development and optimization. Together, these results make this workflow an excellent choice for the routine sequence confirmation and PTM analysis of protein therapeutics.

Methods

Sample preparation: The 10 µg/µL stock solution of NISTmAb (NIST) was diluted in water to 1 µg/µL. The IdeS protease (Promega) in 50 U/µL was added to the diluted NISTmAb solution, and the mixture was incubated at 37°C for 2 hours. After IdeS treatment, a solution of 7.6 M guanidine-hydrochloride (HCl) and 50 mM Tris-HCl (pH=7.4) was added, followed by reduction using dithiothreitol. The mixture was incubated at 60°C for 30 minutes. The reaction was terminated by adding 10% formic acid (FA). The final solution contained ~0.25 µg/µL of the Fc/2, LC, and Fd subunits. A 5 µL final solution (1.25 µg) was injected for LC-MS analysis.

Chromatography: The IdeS subunits of NISTmAb were separated using an ACQUITY UPLC Protein BEH C4 column (2.1 × 50 mm, 1.7 µm, 300 Å, Waters) with the gradient displayed in Table 1. A flow rate of 0.3 mL/min was used for the peptide separation. The column was kept at 60°C in the column oven of an ExionLC system (SCIEX). Mobile phase A was 0.1% FA in water and mobile phase B was 0.1% FA in acetonitrile.

Table 1. LC gradient for peptide separation.

Time (min)	A (%)	B (%)
Initial	80	20
2	80	20
9	55	45
10	10	90
12	10	90
12.5	80	20
15	80	20

Mass spectrometry: MRM^{HR} EAD experiments were performed in SCIEX OS software using the ZenoTOF 7600 system. Three charge states per subunit were targeted for EAD fragmentation in the MRM^{HR} experiments. The key TOF MS and MRM^{HR} settings are listed in Tables 2 and 3, respectively.

Data processing: MRM^{HR} data were analyzed using a new top-down workflow template in the Biologics Explorer software. Three separate workflows with different RT range restrictions were created for the Fc/2, LC, and Fd subunits, respectively. The Lys-loss modification was set on the protein C-terminus of the Fc/2 subunit. The G0F or G1F glycan was specified for the Asn residue in position 61. For the Fd subunit, the Gln to pyro-Glu modification was specified for the N-terminus. The *a*, *b/y*, and *c/z* fragments with a mass tolerance of 20 ppm were considered for fragment mapping. A default maximum intensity of 50 was used

to filter the result of fragment mapping before the percent bond coverage was calculated.

Table 2. TOF MS parameters.

Parameter	Value
Spray voltage	5,500 V
TOF start mass	500 m/z
TOF stop mass	3,000 m/z
Accumulation time	0.2 s
Source temperature	400°C
Declustering potential	80 V
Collision energy	10 V
Time bins to sum	8

Table 3. MRM^{HR} parameters using EAD.

Parameter	EAD
Start mass	100 m/z
Stop mass	3,000 m/z
Q1 resolution	Low
Zeno trap	ON
Zeno threshold	100,000 cps
Accumulation time	0.1 s
Declustering potential	80 V
CE	12 V
Time bins to sum	8
Electron beam current	5,000 nA
Electron KE	1 eV
ETC	100%
Reaction time	5 ms
EAD RF	150 Da

Overview of the EAD-based middle-down workflow

Middle-down MS has been increasingly applied to sequence confirmation and PTM analysis of protein therapeutics for the simplicity of its sample preparation and the high sequence coverage that this approach offers.²⁻⁴ Traditional middle-down MS workflows require extensive method optimization and often involve multiple fragmentation techniques and/or multiple injections with different parameters to achieve optimal sequence coverage.²⁻⁴ These obstacles make it challenging to implement middle-down approaches for routine analysis of protein therapeutics. In this work, a streamlined EAD-based middle-down workflow was developed to provide high sequence coverages of mAb subunits in a single injection using a single fragmentation technique with minimal effort needed for method development and optimization.

Figure 2 shows the EAD-based middle-down workflow from sample preparation to data acquisition and analysis. The workflow starts with IdeS digestion of NISTmAb followed by DTT reduction to generate the Fc/2, LC and Fd subunits. The chromatographic conditions employed in this work provided a consistent baseline separation of the 3 subunits. Intact mass measurement performed using Biologics Explorer software confirmed the masses of 3 major glycoforms of the Fc/2 subunit (G0F, G1F and G2F), the unmodified LC subunit and the Fd

subunit carrying the N-terminal Gln to pyro-Glu modification with high accuracies (mass error < 10 ppm; data not shown). The Zeno EAD offers fast scan rate to allow the fragmentation of multiple charge states of each subunit using the same or different EAD parameters in a single MRM^{HR} method without compromising the data quality. This method generated 1 high-quality data file that provided high sequence coverages (70%-80%) of 3 subunits in a single sample injection. The analysis of middle-down data was performed using an intuitive middle-down workflow template in Biologics Explorer software, which offers powerful tools for spectral annotation, fragment mapping and result review, as will be described in the next section.

Middle-down data analysis using Biologics Explorer software

Biologics Explorer software provides an intuitive middle-down workflow template (Figure 3), which consists of 5 main components. These components include 1) RT and m/z range restrictions to select the MRM data of interest, 2) MS/MS data consolidation and processing to obtain an averaged spectrum, 3) detection and clustering of isotopic profiles in the averaged spectrum using advanced algorithms, 4) fragment mapping to annotate isotopic clusters and achieve a bond cleavage map, and 5) results review and data export. This workflow template was optimized for SCIEX QTOF data and requires minimal user

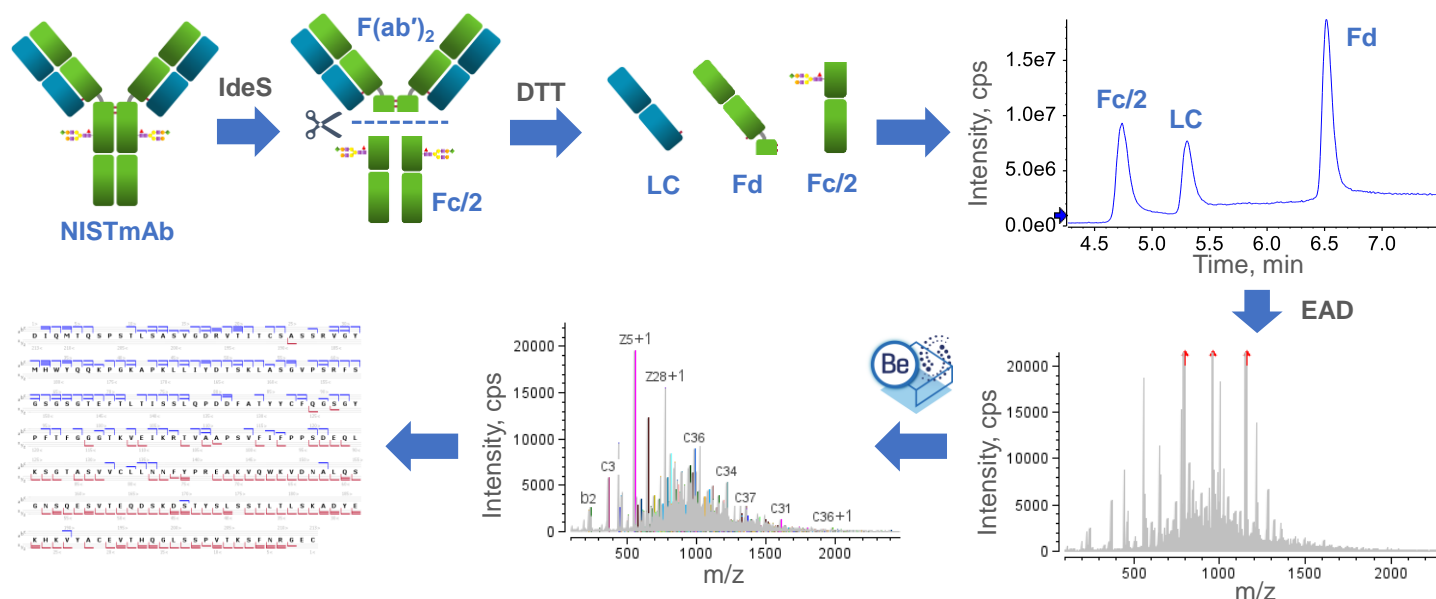


Figure 2. Schematic illustration of the EAD-based middle-down workflow from sample preparation to data acquisition and analysis. In the EAD-based middle-down workflow, the intact NISTmAb was digested by the IdeS protease into the F(ab')₂ and Fc/2 subunits, followed by DTT reduction to produce the Fc/2, LC and Fd subunits. The 3 subunits were chromatographically separated and then targeted for EAD fragmentation in MRM^{HR} experiments. The EAD MS/MS spectra of subunits were interpreted and annotated by Biologics Explorer software to measure the sequence coverages.

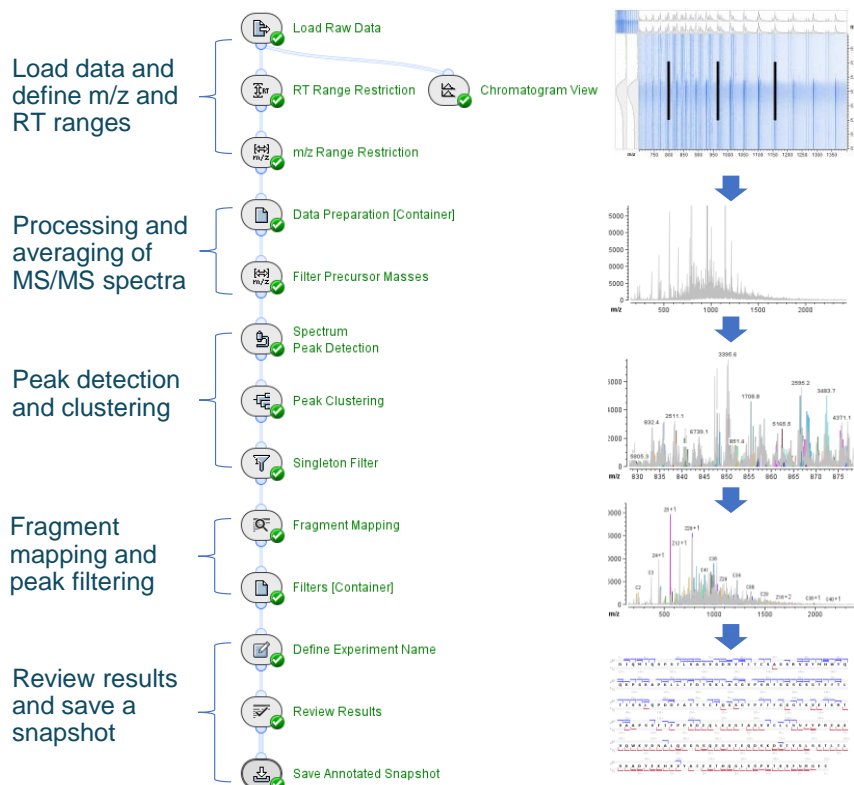


Figure 3. Intuitive middle-down workflow template in Biologics Explorer software. The workflow template contains 5 main components, including data definition, spectrum processing, peak detection and clustering, fragment mapping and results review.

input. In addition to defining the RT and m/z ranges and specifying the sequence and modifications of interest, the user determines the filtering criteria (Step 4), such as the absolute or percentage maximum intensity, based on the signal-to-noise level of the data. While the middle-down workflow template is easy to use, it allows flexibility for advanced users to fine-tune parameters within each activity.

EAD-based middle-down analysis of NISTmAb subunits

EAD provides excellent and reproducible fragmentation of mAb subunits, and sensitive detection of the fragments across different m/z ranges, leading to high sequence coverage in a single injection. In addition, the EAD-based middle-down approach requires minimal time and effort for method optimization, which will be reported in a separate technical note. These advantages of EAD make it an excellent fragmentation technique for middle-down analysis of mAb subunits in different phases of biotherapeutics characterization.

Figure 4 displays the high-quality EAD spectrum acquired for the NISTmAb LC subunit. Many fragments were detected in the scan

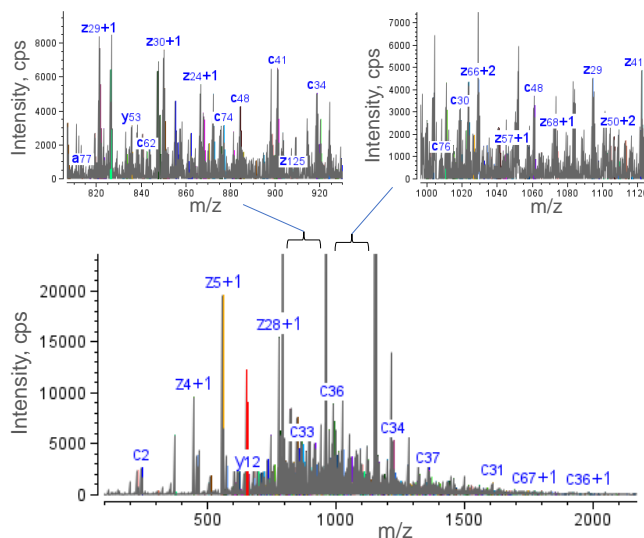


Figure 4. Averaged EAD spectrum of the NISTmAb LC subunit. EAD led to excellent fragmentation of the 3 IdeS subunits of NISTmAb, producing a wealth of fragments in different m/z ranges. The 2 zoomed-in spectra highlight rich sequence fragments that were detected in the 2 selected mass ranges. Not all annotations are shown for spectral clarity.

range, particularly in the m/z range of 500-1,500. The presence of rich fragments is highlighted in two selected mass windows (m/z ~820-920 and ~1,000-1,140) in the 2 insets of Figure 4.

The detection of rich EAD fragments led to high sequence coverages of 78%, 81% and 72% for Fc/2 G0F, LC and Fd, respectively (Figure 5). Sequence coverage of >70% was also achieved for the G1F glycoform of the Fc/2 subunit (data not shown). The measured sequence coverages were comparable to or better than those obtained using multiple injections and/or using multiple fragmentation techniques²⁻⁴, demonstrating the effectiveness of EAD for middle-down analysis in a single injection.

The EAD-based middle-down workflow can provide high sequence coverage of mAb subunits in a single injection, reproducibly between runs. Figure 6 shows the sequence coverages achieved for the Fc/2, LC and Fd subunits across 6 replicate injections. Consistently high sequence coverages (>70%) of the 3 subunits were obtained from these injections, with averaged sequence coverages of 75%, 80% and 72% for the Fc/2, LC and Fd subunits, respectively.

The exceptional sequence coverages obtained for NISTmAb subunits enabled in-depth PTM analysis. Figure 7 shows a selected charge state of the non-glycosylated C_{60} and glycosylated C_{61} fragments. The detection of these fragments enabled the localization of N-glycosylation to Asn⁶¹ in the Fc/2

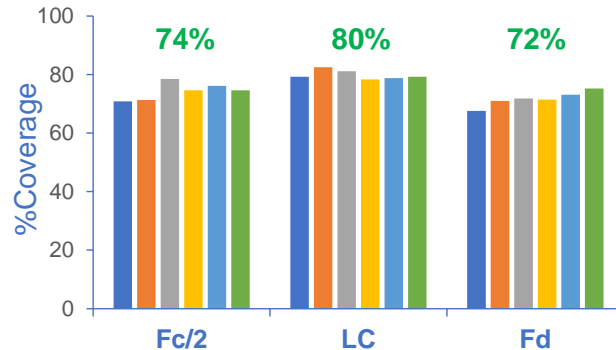


Figure 6. Percent sequence coverages of the Fc/2, LC and Fd subunits from 6 replicate injections. The percent sequence coverages shown above the bar chart are averaged values measured across 6 replicate injections. EAD led to consistently high sequence coverages of the Fc/2, LC and Fd subunits of NISTmAb between runs, demonstrating the effectiveness and reproducibility of this fragmentation approach for the middle-down analysis of mAbs.

subunit. For the Fd subunit, the presence of *c*-series fragments confirmed the Gln to pyro-Glu modification at the N-terminus.

In summary, these results demonstrate that EAD-based middle-down workflow is powerful for sequence and PTM confirmation of mAbs.

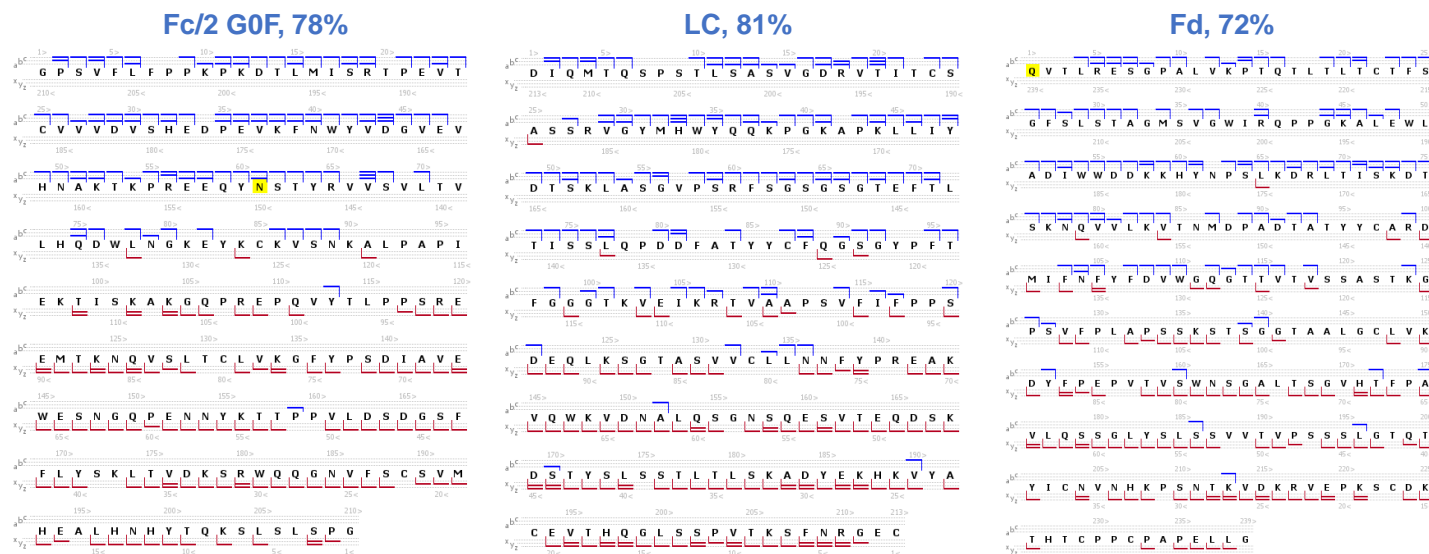


Figure 5. Percent sequence coverages of the Fc/2 G0F, LC and Fd subunits of NISTmAb obtained from a single injection using the EAD-based middle-down workflow. Excellent EAD fragmentation led to high sequence coverages of the Fc/2 G0F (78%), LC (81%) and Fd (72%) subunits in a single injection. The amino acid residues highlighted in the sequences of the Fc/2 and Fd subunits carried modifications. Specifically, the Asn residue in position 61 of the Fc/2 subunit was N-glycosylated whereas the N-terminal Gln in the Fd subunit was converted into a pyroglutamic acid.

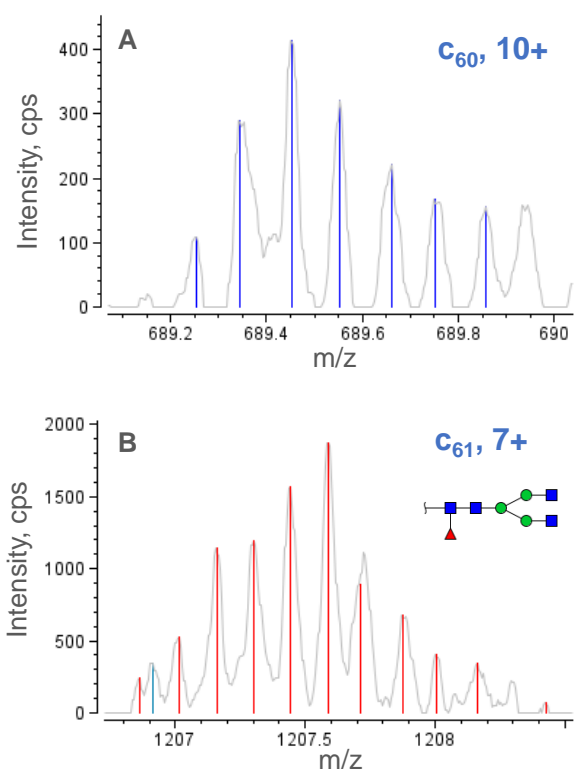


Figure 7. Signature EAD fragments of the Fc/2 G0F subunit confirmed the site of N-linked glycosylation. The detection of non-glycosylated c_{60} and N-glycosylated c_{61} fragments confirmed the site of glycosylation on Asn⁶¹.

Conclusions

- A streamlined EAD-based middle-down workflow enabled confident sequence confirmation and PTM analysis in a single injection
- High sequence coverages ranging from 70 to 80% were obtained for the Fc/2, LC and Fd subunits of NISTmAb in a single injection and consistently between runs
- PTMs of the Fc/2 and Fd subunits were confidently confirmed based on the detection of signature ions from excellent EAD fragmentation
- Biologics Explorer software offers an easy-to-use and optimized workflow template for improved user experience with middle-down data analysis

The SCIEX clinical diagnostic portfolio is For In Vitro Diagnostic Use. Rx Only. Product(s) not available in all countries. For information on availability, please contact your local sales representative or refer to www.sciex.com/diagnostics. All other products are For Research Use Only. Not for use in Diagnostic Procedures.

Trademarks and/or registered trademarks mentioned herein, including associated logos, are the property of AB Sciex Pte. Ltd. or their respective owners in the United States and/or certain other countries (see www.sciex.com/trademarks).

© 2023 DH Tech. Dev. Pte. Ltd. MKT-26997-A

References

1. Anna Robotham and John Kelly. (2020) LC-MS characterization of antibody-based therapeutics: recent highlights and future prospects. [Approaches to the Purification, Analysis and Characterization of Antibody-Based Therapeutics. Chapter 1: 1-33.](#)
2. Milos Cejkov et al. (2021) Electron transfer dissociation parameter optimization using design of experiments increases sequence coverage of monoclonal. [J. Am. Soc. Mass Spectrom. 32\(3\): 762-771.](#)
3. Luca Fornelli *et al.* (2018) Accurate sequence analysis of a monoclonal antibody by top-down and middle-down Orbitrap mass spectrometry applying multiple ion activation techniques. [Anal. Chem. 90\(14\): 8421-8429.](#)
4. Kristina Srzentic *et al.* (2020) Interlaboratory study for characterizing monoclonal antibodies by top-down and middle-down mass spectrometry. [J. Am. Soc. Mass Spectrom. 31\(9\): 1783-1802.](#)

Direct and rapid multi-attribute monitoring of multiple intact monoclonal antibodies with a wide isoelectric-point range of 7.3 to 9.1

Featuring an imaged capillary isoelectric focusing (icIEF)-UV/MS workflow using the Intabio ZT system from SCIEX

Scott Mack, Zhichang Yang, Zoe Zhang, Rita Nichiporuk, and Maggie Ostrowski
SCIEX, USA

This technical note demonstrates a novel integrated workflow using the Intabio ZT system. This innovative system offers direct chip-based integration of icIEF with mass spectrometry (MS), which affords confident characterization of different proteoforms of biotherapeutics and reliable quantitation of charge variants. Further, the streamlined icIEF-UV/MS platform significantly reduces the time to results from weeks to approximately 1 hour for routine samples, compared to ion exchange chromatography (IEX) with fraction collection.¹

Recombinant monoclonal antibodies (mAbs) have become an important class of biotherapeutics to treat various diseases due to their high specificity and efficacy.² During the manufacturing process, heterogeneity can occur in mAbs due to enzymatic cleavage and chemical post-translational modifications (PTM).³ Many PTMs, including deamidation, C-terminal lysine truncation, glycation and sialylation, change the isoelectric point (pI) of a mAb.⁴ Characterizing the charge heterogeneity of mAbs is therefore important for critical quality attribute (CQA) assessment to ensure drug safety, efficacy and potency.⁵ In addition, process changes can occur during manufacturing, which poses a

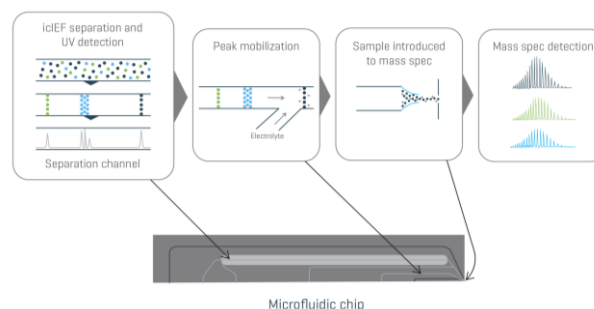


Figure 2. icIEF-UV/MS analysis on the Intabio ZT system

significant concern for the development of biopharmaceutical therapeutics, as process changes could result in PTMs that impact product quality.

cIEF offers high-resolution separation of protein charge variants, including compounds with similar pI values.⁶ Therefore, cIEF is commonly used to monitor charge variant profiles. However, numerous technical challenges inhibit the direct combination of upstream icIEF-UV characterization with downstream identification by mass spectrometry and have limited the ability to identify proteoforms in each charge variant.

In this technical note, a platform assay using the direct chip-based integration of icIEF-UV/MS was employed to characterize 3 mAbs spanning a wide pI range⁷ (Figure 1).

Key features of the icIEF-UV/MS workflow

- Seamless identification of charge variants with a microfluidic chip-based integrated icIEF-UV/MS technology. The Intabio ZT system is exclusively coupled to the ZenoTOF 7600 system.
- This platform offers rapid monitoring and identification of intact biotherapeutics with a wide pI range of 7.3 to 9.1 by icIEF-UV/MS
- The 30-min sample analysis is significantly faster than conventional cIEF and IEX workflows requiring fractionation for the following identification.
- icIEF separation and UV quantitation correlate well with standard icIEF techniques

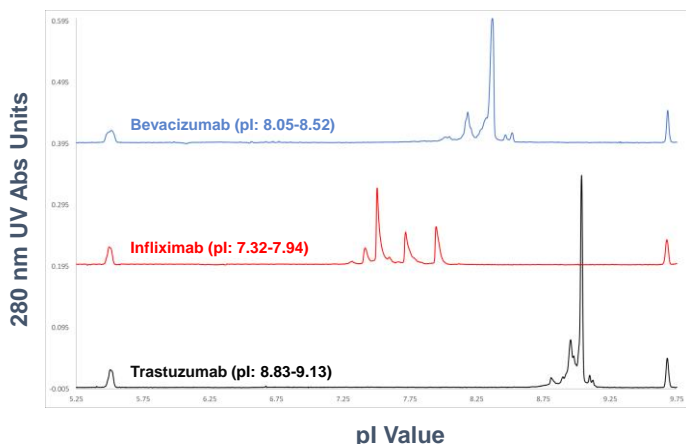


Figure 1. Overlay of icIEF-UV profiles demonstrating separated charge variants for bevacizumab (blue), infliximab (red) and trastuzumab (black) from data acquired with the Intabio ZT system.

- Streamlined, intuitive data analysis software is available for rapid reporting and results sharing

Methods

Equipment: The Intabio ZT system (SCIEX) and Intabio ZT cartridge (SCIEX, P/N 5088248) were used for the separation of the 3 mAbs and their charge variants. MS detection was performed on the ZenoTOF 7600 system (SCIEX, P/N 5080337) equipped with components of the OptiFlow interface (SCIEX, P/N 5084645).

Table 1. icIEF separation parameters.

Hold time (s)	Anode voltage (V)	Cathode setting	Mobilization setting	Step
60	1500	0 V	0 A	Focusing
60	3000	0 V	0 A	Focusing
300	4500	0 V	0 A	Focusing
600	8500	0 A	5500 V	Mobilization

Chemicals and reagents: The Intabio system – Electrolyte and Mobilizer kit (P/N 5088205) was used for anolyte, catholyte and mobilizer. Anolyte and mobilizer were used undiluted. The stock catholyte solution was 1% and diluted to 0.25% for use in the reagent drawer. The stock anolyte is 1% formic acid and catholyte is 1% diethylamine. The mobilizer is composed of 25% acetic acid, 25% acetonitrile and 50% water.

A 500mM cathodic spacer solution containing free base L-Arginine (purity ≥ 98.5%, Sigma-Aldrich, P/N A8094-25G) was prepared by dissolving 0.870 mg of Arg powder into 10 mL of Milli-Q water. The electrolytes and cathodic spacer solutions were stored at room temperature. pI markers (CanPeptide) were individually dissolved in Milli-Q water at 5 mg/mL.

Prior to icIEF-UV/MS analysis, bevacizumab, infliximab, trastuzumab and NISTmAb were desalted with a Zeba Spin Desalting Columns, 7K MWCO, 0.5 mL (Thermo Fisher Scientific, P/N 89882).

Bevacizumab, infliximab and trastuzumab are from stock solutions.

icIEF-UV/MS analysis: The MS signal was optimized before sample analysis using a solution containing 100 µg/mL of NISTmAb in mobilizer solution. The NISTmAb solution was infused through the Intabio ZT cartridge with 100-150 mbar of pressure. Electrospray ionization was achieved into a ZenoTOF 7600 system with a tip voltage between 5000 and 5500 V. Nitrogen gas was applied between 60 and 75 psi to the on-chip integrated nebulization channels that are coplanar with the tip of

the icIEF-UV/MS chip to achieve stable and robust ionization and sample entry to the MS system.

Samples containing 250 µg/mL of NISTmAb, 10mM arginine, 1% Pharmalyte 3 to 10 (Cytiva, P/N 17045601), 2.5% Pharmalyte 8 to 10.5 (Cytiva, P/N 17045501) and 6.25 µg/mL of peptide pI markers were vortexed and then degassed by centrifugation at 3900 rcf.

The streamlined process of icIEF-UV/MS analysis is illustrated in Figure 2. First, 70 psi of nitrogen was supplied to the internal nebulization channel within the Intabio ZT cartridge during the loading, focusing and mobilization cycles of the icIEF-UV/MS separation process. After priming the channels within the Intabio ZT cartridge with either electrolyte solution or water, 50 µL of the sample was automatically loaded onto the separation channel using the autosampler. The icIEF separation was achieved using the parameters shown in Table 1. Absorbance measurements were collected at 1 Hz throughout the focusing and mobilization steps. The samples were introduced into the ZenoTOF 7600 system by a metered 2 µL/min flow of chemical mobilizer, and the data was acquired using parameters shown in Table 2.

Data processing: UV profiles and mass spectra from the icIEF-UV/MS analysis of mAbs were analyzed using the Biologics Explorer software. Each peak in the icIEF-UV profile was integrated to determine peak area and percent composition. Intact masses were estimated from the raw mass spectrum under each peak of the icIEF-MS profile utilizing a charge deconvolution algorithm with a mass range setting between 145,000 and 150,000 Da.

Table 2. TOF MS parameters.

Parameter	Value
Curtain gas	15 psi
Spray voltage	5500 V
TOF start mass	2000 m/z
TOF stop mass	6000 m/z
Accumulation time	0.5 s
Source temperature	100°C
Declustering potential	210 V
Collision energy	55 V
Time bins to sum	150

Results and discussion

Figure 3 shows the icIEF-UV and icIEF-MS profiles of the charge variants of 3 mAbs acquired with the Intabio ZT system coupled to ZenoTOF 7600 system. The left panels show 280 nm UV absorbance profiles of trastuzumab, infliximab and bevacizumab charge variants separated by icIEF. The right panels are MS base peak electropherograms (BPEs) of the corresponding peaks after mobilization, electrospray ionization and detection by MS. The separation profiles generated by icIEF-UV (once inverted) and icIEF-MS on the Intabio ZT system and ZenoTOF 7600 system, respectively, are similar. icIEF-UV profile shows separated peaks across the icIEF separation channel, whereas icIEF-MS profile is acquired based on the time at which the charge variants flow into the MS system after mobilization. Basic peaks on the icIEF-UV profile at high pI are introduced first into the MS system for analysis and therefore appear at earlier points (left side of the MS BPE). The MS BPE shows that all the peaks observed on icIEF-UV profile were also detected in icIEF-MS profile without compromising separation resolution. This result indicates that the separation efficiency of charge variants was well-maintained after chemical mobilization. The entire focusing and separation step took less than 15 minutes, demonstrating the capability of this workflow for high-throughput analysis.

Quantitation of charge variants

The percent composition of acidic, basic and main peaks in the icIEF-UV profiles for each mAb analyzed is shown in Table 3. The use of the Intabio ZT system allowed quantitative information of the mAb charge variants to be successfully obtained from icIEF-UV profile while the proteoform composition of the charge variant peaks was identified by the coupled ZenoTOF 7600 system.

Characterization of charge variants

A detailed characterization of the charge variant peaks was performed for 3 mAbs to identify different proteoforms. Figure 4 shows a summary of the identified PTMs for charge variant peaks from different mAbs (top) and the corresponding deconvoluted mass spectra (bottom). Deamidation and sialylated glycans were detected in the acidic peaks of trastuzumab. Potential glycation (Hex) was observed in main peak b (green), to which other glycan isoforms can contribute. Succinimide was detected in basic peak 1 (dark blue) and C-terminal lysine variants were identified in basic peak 2 (purple). Basic peaks 1 and 2 represented different proteoforms, which differed by only 0.02 pI and were well-separated, demonstrating the high-resolution of icIEF separation on the Intabio ZT system. For infliximab, deamidation and sialylated glycans were also identified in the acidic peaks (orange). C-terminal lysine variants were identified in both basic

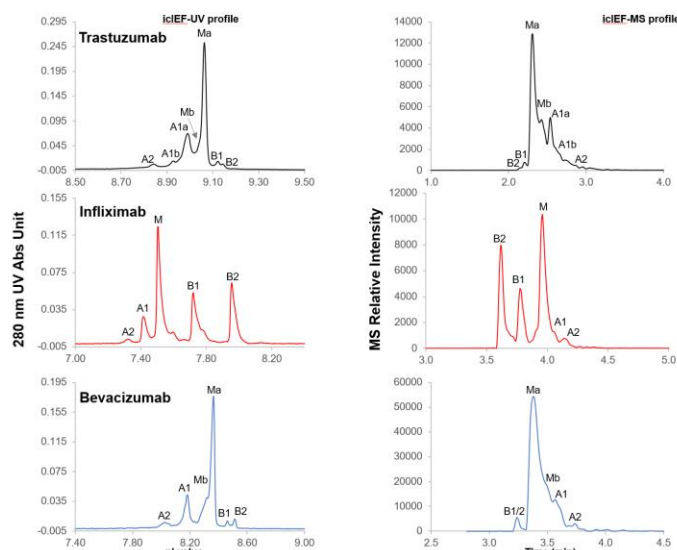


Figure 3. Trastuzumab, infliximab and bevacizumab intact charge profiles. The left panel shows icIEF-UV profiles of trastuzumab, infliximab and bevacizumab charge variant separation, in the scale of the pI value (x axis) acquired from the Intabio ZT system. The right panel shows the MS BPE of mAb charge variants acquired from ZenoTOF 7600 system after icIEF separation.

peaks 1 (1 Lys) and 2 (2 Lys), which are illustrated in dark blue and purple traces, respectively. For bevacizumab, deamidation were observed in both acidic peaks (yellow and red) and the main peak b (green). C-terminal lysine variants were the major species detected in the basic peaks (dark blue and purple). In addition, icIEF-UV profile reveals the existence of low-level pyroglutamate in basic peak 1. Additional complex glycans were identified by icIEF-MS profile for all 3 mAbs as listed in the figures, covering a wide range of pI values. The 3 mAbs with different pI values were comprehensively characterized by a platform method, demonstrating the user-friendly operation of the icIEF-UV/MS system without redundant method development for different molecules.

Table 3. Percent composition (%) of 3 mAbs.

	Trastuzumab	Infliximab	Bevacizumab
Acidic group	39.73	13.89	48.78
Main group	54.07	34.85	43.30
Basic group	6.20	51.25	7.93

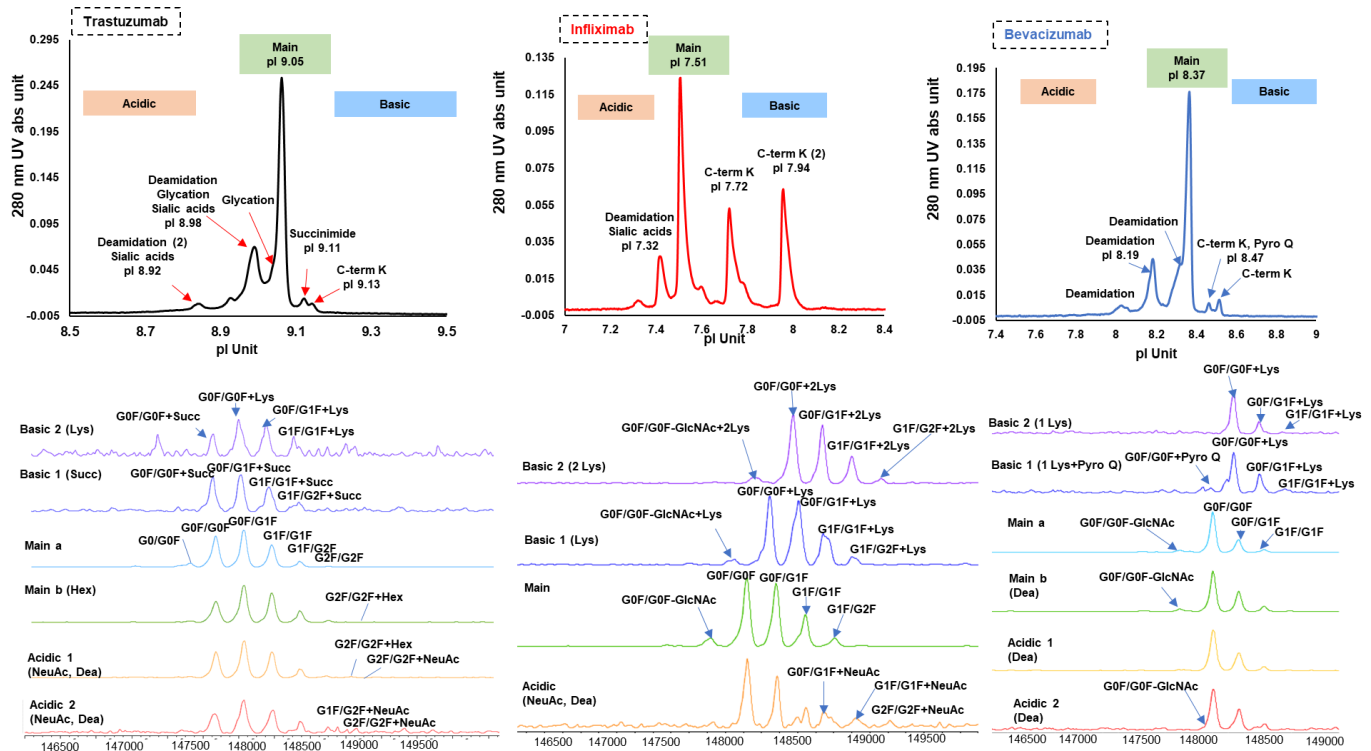


Figure 4. Detailed analysis of the charge variant peaks of the 3 mAbs. The upper panels show the icIEF-UV profiles achieved for trastuzumab (left), infliximab (middle) and bevacizumab (right). These data were acquired using the Intabio ZT system and were in the scale of the pI value (x axis). The PTMs identified for specific peaks of each charge variants are annotated. The lower panels are an overlay of the intensity normalized deconvoluted mass spectrum of the charge variants, showing the identity of the peaks detected in the icIEF-UV/MS analysis; the data analysis was performed by the Biologics Explorer software.

Figure 5 shows an example of the analysis results obtained using the Biologics Explorer software. The layout simultaneously

includes the UV electropherogram, results summary, MS data, deconvoluted ion map results and raw MS data. On the top left

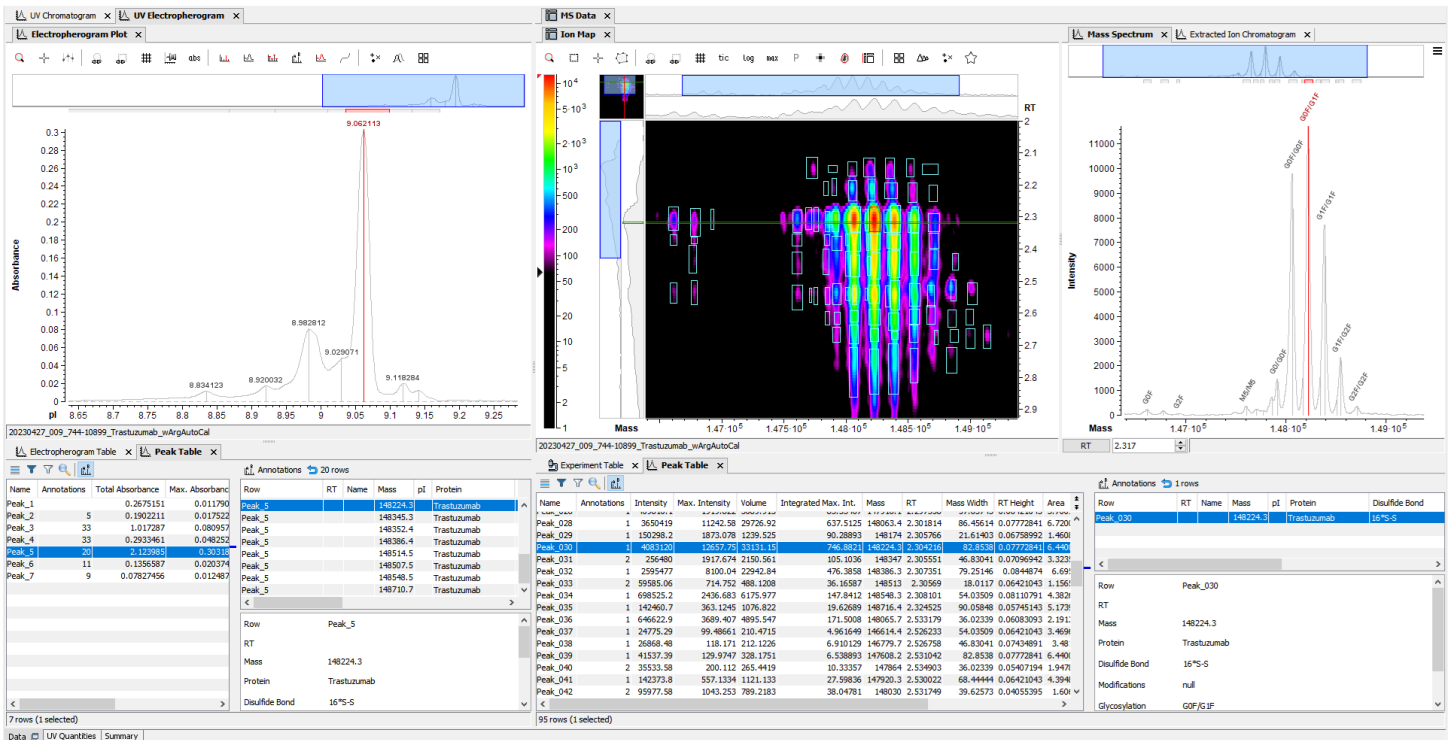


Figure 5. The report interface from Biologics Explorer software.

panel, the UV electropherogram is illustrating the isoelectric focusing separation of charge variants and the integration of identified peaks. Peaks identified in the icIEF-UV profiles (electropherogram table) and MS BPE (peak table) are separately listed in the bottom left panel with detailed annotations of the identified proteoforms in the annotation section. The top right panel presents the ion map (color image) and deconvoluted mass spectra of the peak selected in the left panel. The bottom right panel shows the peak selected in the deconvoluted mass spectra including peak intensities, retention time and method used for data analysis. This report summary demonstrates a comprehensive overview of a streamlined charge variant characterization using the Biologics Explorer software.

Conclusions

- The Intabio ZT system enables a streamlined workflow to separate charge variants by icIEF and identify them with ZenoTOF 7600 system across a pI range of 7.3 to 9.1
- A unified icIEF-UV/MS workflow offers high sensitivity and selectivity to detect low-abundant proteoforms that might impact product quality
- The separation efficiency and resolution of icIEF are well-maintained after mobilization, enabling highly confident identification of CQAs by icIEF-UV/MS, such as C-terminal lysine variants, glycosylation, deamidation and glycation (Hex)
- The Intabio ZT system is a commercially available platform that offers workflow combining icIEF separation, UV quantitation and MS-based identification.

References

1. Ostrowski M. Rapid multi-attribute characterization of intact bispecific antibodies by a microfluidic chip-based integrated icIEF-MS technology. [Electrophoresis. 2022 Oct;1-9](#)
2. Mullard A. FDA approves 100th monoclonal antibody product. *Nat Rev Drug Discov.* [2021 Jul;20\(7\):491-495.](#)
3. Houde D, Peng Y, Berkowitz SA, Engen JR. Post-translational modifications differentially affect IgG1 conformation and receptor binding. *Mol Cell Proteomics.* [2010 Aug;9\(8\):1716-28.](#)
4. Vlasak J, Bussat MC, Wang S, Wagner-Rousset E, Schaefer M, Klinguer-Hamour C, Kirchmeier M, Corvaia N, Ionescu R, Beck A. Identification and characterization of asparagine deamidation in the light chain CDR1 of a humanized IgG1 antibody. *Anal Biochem.* [2009 Sep 15;392\(2\):145-54.](#)
5. Liu H, Ponniah G, Zhang HM, Nowak C, Neill A, Gonzalez-Lopez N, Patel R, Cheng G, Kita AZ, Andrien B. In vitro and in vivo modifications of recombinant and human IgG antibodies. *MAbs.* [2014;6\(5\):1145-54.](#)
6. Hühner J, Lämmerhofer M, Neusüß C. Capillary isoelectric focusing-mass spectrometry: Coupling strategies and applications. *Electrophoresis.* [2015 Nov;36\(21-22\):2670-2686.](#)
7. Bumbaca D, Boswell C, Fielder P, Khawli L. Physicochemical and Biochemical Factors Influencing the Pharmacokinetics of Antibody Therapeutics. *AAPS J.* [2012 Sep 14\(3\):554-558](#)

The SCIEX clinical diagnostic portfolio is For In Vitro Diagnostic Use. Rx Only. Product(s) not available in all countries. For information on availability, please contact your local sales representative or refer to www.sciex.com/diagnostics. All other products are For Research Use Only. Not for use in Diagnostic Procedures.

Trademarks and/or registered trademarks mentioned herein, including associated logos, are the property of AB Sciex Pte. Ltd. or their respective owners in the United States and/or certain other countries (see www.sciex.com/trademarks). Intabio is being used under license.

© 2023 DH Tech. Dev. Pte. Ltd. MKT-26996-A



Headquarters
 500 Old Connecticut Path | Framingham, MA 01701 USA
 Phone 508-383-7700
sciex.com

International Sales
 For our office locations please call the division headquarters or refer to our website at sciex.com/offices

Lightning capillary electrophoresis sodium dodecyl sulfate (CE-SDS) workflow for high-throughput analysis of biotherapeutics

Zhichang Yang, Marcia Santos, Tingting Li, Mario Pulido, Jane Luo and Sahana Mollah
SCIEX, USA
Biopharma

Introduction

There are hundreds to thousands of drug candidates to screen during early drug development, posing a considerable bottleneck in the biopharma industry. High-throughput analytical platforms and fast analysis methods are attractive approaches to help solve the high sample volume issue. CE-SDS is the gold-standard method widely used for drug purity, integrity and stability analysis. However, this need is not met with the current single-capillary system. In this technical note, we propose the lightning CE-SDS workflow, which, together with a multi-capillary system, this workflow speeds up separation to 1.5 x faster than SCIEX gold standard CE-SDS workflow (Figure 1). This method can analyze 192 reduced samples in 14 hours (4.3 min/sample) with high data quality. The relative standard deviation (RSD) % of relative migration time (RMT) and corrected peak area (CPA) % across 192 injections are below 1% and 3%, respectively. Through a systematic evaluation of multiple variables in only 6 days, we proved the high accuracy and separation efficiency with no carryover.

During early drug development, screening a large number of clones for lead clone selection is a critical step in cell line development. This process can be time-consuming and a labor-intensive process without high-throughput methodology.¹



Meanwhile, developability assessment studies, as a screening strategy to identify process development issues associated with product stability, purity and integrity, require robust and fast analytical approaches to redirect resources to more promising products.² To this point, CE-SDS is widely used in biotherapeutics analyses for lot release, stability testing, formulation-buffer screening, process development, cell line development and product characterization. CE-SDS is an automation-friendly application that when combined with a robust multi-capillary electrophoresis system that offers high-throughput, becomes a powerful analytical tool for product characterization during process and cell line development.³ In this technical note, we increased the throughput on the CE-SDS workflow, enabling the analysis of 192 injections (2 full 96-well plates worth of samples) of IgG standard under reduced (R) and non-reduced (NR) conditions in 14 and 18 hours, respectively, with remarkable reproducibility. This study demonstrates that lightning CE-SDS is accurate and precise as the original workflow with no carryover or loss of separation efficiency.

Key features

- The lightning CE-SDS workflow is up to 1.5 x faster than SCIEX original CE-SDS workflow enabling the analysis of 192 injections of IgG standard in reduced and non-reduced condition within 14 and 18 hours, respectively. That equals to 4.3 min and 5.5 min per injection.
- Exceptional repeatability over 192 injections was achieved with < 1% RSD% and < 3% RSD of relative MT and CPA%, respectively, for all major peaks of IgG standard
- Highly robust workflow with excellent intermediate precision, accuracy and no carryover or loss of separation efficiency

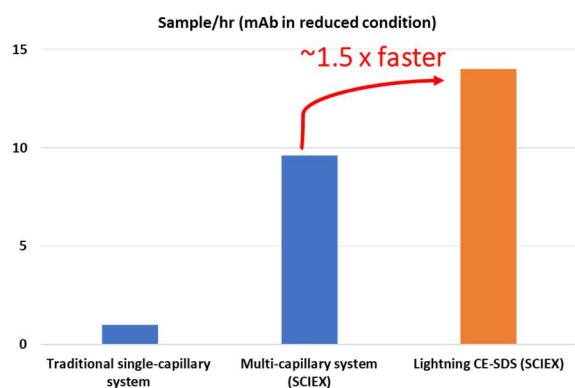


Figure 1. Throughput capability achieved by lightning CE-SDS compared to validated gold-standard workflows.

Materials and methods

Chemicals: IgG control standard (PN: 391734) and CE-SDS Protein Analysis Kit (PN: C30085) and the IgG control standard (PN 391734) were from SCIEX, (Framingham, MA). The NIST mAb (RM 8671) reference material 8671 was from NIST (Gaithersburg, MD). The iodoacetamide (PN: I6125-5G) and the 2-mercaptoethanol (PN: M3148-25ML) were from Sigma Aldrich (St. Louis, MO). Chromeo P503 dye (PN: 15106) was from Active Motif, Inc (Carlsbad, CA).

Materials and instruments: BioPhase 8800 system (PN: 5083590F) equipped with UV absorbance detection at 220 nm and LIF detector with 488 nm excitation and 600 nm emission. BioPhase BFS capillary cartridge - 8 x 30 cm (PN: 5080121) and Sample and Reagent Plates (PN: 5080311) were from SCIEX (Framingham, MA). Multi-Therm shaker incubator (Part # H5000-H) was from Benchmark Scientific (Sayreville, NJ). 600 nm/80 nm bandpass filter FWHM 12.5 mm (PN 65736) was from Edmond Optics Worldwide (Barrington, NJ).

Sample preparation for CE-SDS analysis using UV

detection: The IgG control standard was prepared by adding 16 μL of 10 kDa Internal Standard and 40 μL of 250 mM iodoacetamide (IAM) for non-reduced sample or β -mercaptoethanol (β -ME) for the reduced sample to 760 μL of the IgG control standard solution. The sample mixture was vortexed, centrifuged and then heat denatured at 70°C for 10 min. The sample was then cooled to room temperature and 100 μL aliquots were transferred to the 8 wells of the sample plate for CE-SDS analysis. The NIST reference standard was prepared by adding 995 μL SDS-MW sample buffer, followed by adding of 25 μL of 10kD, 60 μL of 250 mM IAM for non-reduced sample or β -ME for reduced sample to 120 μL of 10mg/mL NIST. The sample mixture was vortexed, centrifuged and then heat denatured at 70°C for 10 min. The final concentration of NIST reference standard was 1 mg/mL.

Sample preparation for CE-SDS analysis using LIF

detection: 12 μL of 10 mg/mL NIST mAb was added to 1128 μL SDS-MW sample buffer, followed by either 60 μL of 250 mM IAM for non-reduced sample or β -ME for reduced sample. The sample mixture was vortexed, centrifuged and then heat denatured at 70°C for 10 min. After cooling down to room temperature, 4 μL Chromeo P503 dye (1 mg/mL) was added to the sample. The sample mixture was vortexed, centrifuged and then heated at 70°C for 10 min for fluorescent labeling. The final concentration of NIST mAb for CE-SDS-LIF analysis is 0.1 mg/mL.

50 μL of treated NIST mAb was transferred to the sample plate for CE-SDS analysis (UV and LIF). Figure 2 shows the sample plate layout used in the systematic study.

CE methods: Figures 3, 4 and 5 show the cartridge conditioning, original sample separation and the lightning CE-SDS separation methods used in this work.

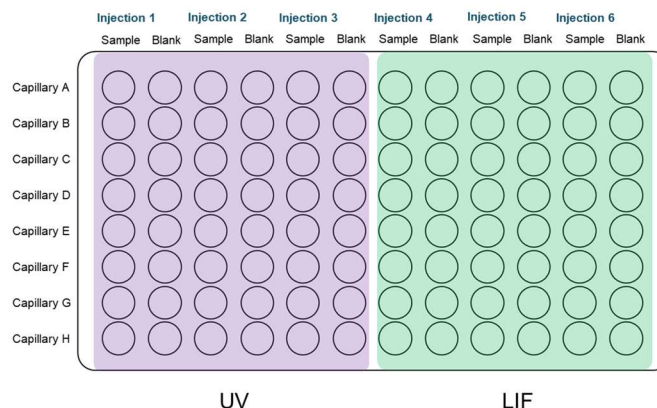


Figure 2. Layout of the sample plate for 1 analysis run of the systematic study.

Method Duration: 37.0 min Number of Actions: 7









	Settings	Capillary Cartridge: 25.0 °C Capillary Length: 30.0 cm Capillary Type: Bare Fused Silica Current Limit: 600 μA , Enabled	Sample Storage: 25.0 °C Detector Type: UV, 220 nm Peak Width: 2 sec Data Rate: 4 Hz
	Rinse	Duration: 2.0 min 70.0 psi	Inlet: 0.1 N NaOH Outlet: Waste
	Rinse	Duration: 8.0 min 20.0 psi	Inlet: 0.1 N NaOH Outlet: Waste
	Rinse	Duration: 5.0 min 20.0 psi	Inlet: 0.1 N HCl Outlet: Waste
	Rinse	Duration: 2.0 min 20.0 psi	Inlet: Water Rinse Outlet: Waste
	Rinse	Duration: 10.0 min 80.0 psi	Inlet: SDS Gel Rinse Outlet: Waste
	Separate	Duration: 10.0 min -15.0 kV, 20.0 psi, Both Ramp time: 5.0 min	Inlet: SDS Gel Sep Outlet: SDS Gel sep
	Wait	Duration: 0.0 min	Inlet: Water Dip 1 Outlet: Water Dip

Figure 3. Screenshot of cartridge conditioning method.

Method Duration: 60.3 min Number of Actions: 11

Settings	Capillary Cartridge: 25.0 °C Capillary Length: 30.0 cm Capillary Type: Bare Fused Silica Current Limit: 600 µA, Enabled	Sample Storage: 25.0 °C Detector Type: UV, 220 nm, Wait Peak Width: 2 sec Data Rate: 4 Hz
Rinse	Duration: 2.0 min 80.0 psi	Inlet: 0.1 N NaOH Outlet: Waste
Rinse	Duration: 5.0 min 20.0 psi	Inlet: 0.1 N NaOH Outlet: Waste
Rinse	Duration: 5.0 min 20.0 psi	Inlet: 0.1 N HCl Outlet: Waste
Rinse	Duration: 3.0 min 20.0 psi	Inlet: Water Rinse Outlet: Waste
Rinse	Duration: 10.0 min 80.0 psi	Inlet: SDS Gel Rinse Outlet: Waste
Wait	Duration: 0.0 min	Inlet: Water Dip 1 Outlet: Water Dip
Wait	Duration: 0.0 min	Inlet: Water Dip 2 Outlet: Water Dip
Inject	Duration: 20 sec -5.0 kV	Tray: Sample Outlet: SDS Gel Inj
Wait	Duration: 0.0 min	Inlet: Water Dip 3 Outlet: Water Dip
Separate	Duration: 35.0 min -15.0 kV, 20.0 psi, Both Ramp time: 2.0 min Autozero: 0.1 min	Inlet: SDS Gel Sep Outlet: SDS Gel sep
Wait	Duration: 0.0 min	Inlet: Water Dip 1 Outlet: Water Dip

Figure 4. Screenshot of CE-SDS original separation method (for non-reduced antibody analysis condition). Separation time is set to 25 min for reduced antibody analysis.

Method Duration: 44.3 min Number of Actions: 10

Settings	Capillary Cartridge: 25.0 °C Capillary Length: 30.0 cm Capillary Type: Bare Fused Silica Current Limit: 600 µA, Enabled	Sample Storage: 25.0 °C Detector Type: UV, 220 nm, Wait Peak Width: 2 sec Data Rate: 4 Hz
Rinse	Duration: 2.0 min 80.0 psi	Inlet: 0.1 N NaOH Outlet: Waste
Rinse	Duration: 2.0 min 50.0 psi	Inlet: 0.1 N HCl Outlet: Waste
Rinse	Duration: 1.0 min 50.0 psi	Inlet: Water Rinse Outlet: Waste
Rinse	Duration: 4.0 min 80.0 psi	Inlet: SDS Gel Rinse Outlet: Waste
Wait	Duration: 0.0 min	Inlet: Water Dip 1 Outlet: Water Dip
Wait	Duration: 0.0 min	Inlet: Water Dip 2 Outlet: Water Dip
Inject	Duration: 20 sec -5.0 kV	Tray: Sample Outlet: SDS Gel Inj
Wait	Duration: 0.0 min	Inlet: Water Dip 3 Outlet: Water Dip
Separate	Duration: 35.0 min -15.0 kV, 20.0 psi, Both Ramp time: 2.0 min Autozero: 0.1 min	Inlet: SDS Gel Sep Outlet: SDS Gel sep
Wait	Duration: 0.0 min	Inlet: Water Dip 1 Outlet: Water Dip

Figure 5. Screenshot of lightning CE-SDS separation method (for non-reduced antibody analysis condition). Separation time is set to 25 min for reduced antibody analysis.

The rinse cycles in the lightning CE-SDS method has been reduced to only 9 min while maintaining all the rinsing reagents. That reduced the total separation time by 64% compared to the original workflow.

Data analysis: The BioPhase analysis software package version 1.0 was used to create methods and sequences followed by data acquisition (not data analysis) and data processing.

Results and discussions:

The high-throughput capabilities of the lightning CE-SDS

workflow: To increase throughput by reducing the cycle time of CE-SDS analysis while maintaining separation efficiency and workflow robustness is critical to retaining high data quality. The rinsing time in the SCIEX original workflow takes up to 50% of the total cycle time. One strategy to reduce the cycle time is by reducing the rinsing time. However, for a thorough capillary surface cleaning and conditioning, we only reduced the duration of the rinse steps while keeping all necessary reagents used in the current method. The combination of high pressure (Figure 5) allows for effective capillary surface treatment while reducing the overall rinsing time to only 9 minutes, or 64% compared to the original workflow. As a result, the separation efficiency and migration time requirements remain the same as the original CE-SDS workflow. Table 1 summarizes the throughput results for the lightning and the original CE-SDS workflows. The lightning CE-SDS workflow took only 6.9 and 8.8 hours to complete one 96-well plate for reduced and non-reduced IgG control standards, translating into an average of 14 reduced and 11 non-reduced samples/hr.

Table 1. Throughput result of lightning and original CE-SDS workflow.

Condition	Workflow	Cycle time	Min/Sample*	Hrs/Plate	Samples/hr
Reduced	Lightning	34 min	4.3	6.9	14
	Original	50 min	6.25	10	9
Nonreduced	Lightning	44 min	5.5	8.8	11
	Original	60 min	7.5	12	8

*min/sample acquired by cycle time divided by 8

To determine the reproducibility of the lightning CE-SDS workflow, we performed 24 consecutive injections of IgG control standard from 1 column of sample plate, that is 8 samples injected 24 times for a total of 192 injections, under reduced and non-reduced conditions. Figure 6 highlights the separation consistency of the lightning CE-SDS workflow. The separation profiles between the first and 24th injection were comparable, indicating that the reduced rinsing conditions did not compromise the separation efficiency.

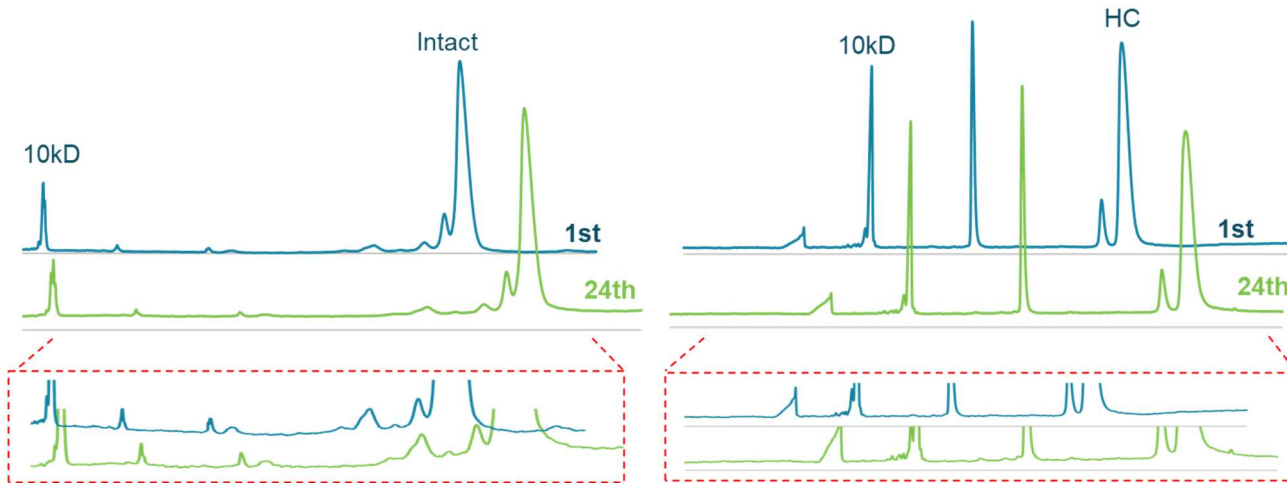


Figure 6. The separation profile comparison between 1st and 24th injection of IgG control standard under non-reduced (left panel) and reduced (right panel) conditions. The figures inside the red blocks showcase the consistency of the profiles at the baseline level for each separation.

To quantify the consistency of the lightning CE-SDS workflow, we calculated the RSD% (N=192) of relative migration time (RMT) and corrected peak area (CPA) % of the major peaks such as, light chain (LC), heavy chain (HC), non-glycosylated heavy chain (NG-H) of the reduced IgG and HC:HC:LC (HHL) and intact IgG peak of non-reduced IgG. As shown in Figure 7, the RSD% for RMT was below 0.5% for all major peaks. The

RSD% for CPA% was < 1.5% for reduced IgG control peaks and < 2.5% for non-reduced IgG control peaks. The low RSD% of both figures of merit indicates the high reproducibility of the workflow. Most notably, the minor species such as, NG-H and HHL achieved RSD% of less than 3% over 192 replicates for CPA%.

Validation of the Lightning CE-SDS workflow by multiple factorial design using NIST reference standard mAb:

Because of the multi-capillary environment of the BioPhase 8800 system, to better understand the study design and the data output this platform can generate in 1 sequence, the terms used in this work are defined as follows. Data point refers to one separation from 1 well using 1 capillary. Each run refers to 8 data points. The sample plate layout (Figure 2) used in this work comprises 3 columns (or 8 samples) for UV detection and 3 columns of samples for LIF detection. Between each column of samples, a column of sample buffer is used as blanks to assess carryover. One sequence is defined as a single separation of 1 sample (NIST antibody) plate with the layout on Figure 2, generating 48 datapoints. Table 2 illustrates the experimental design to evaluate the robustness of the lightning CE-SDS workflow. The study required each of the 3 analysts to prepare 1 sample plate daily as described in Figure 2. Each analyst ran different instruments using 3 different cartridges (triplicate runs per plate/day) with 9 runs, generating 432 data points for reduced and non-reduced samples. This study provided insights into variation potentially caused by instruments, analyst operation, cartridges, capillaries and different injections. These multiple factors were effectively tested in triplicates to highlight their impact in the overall results directly. Most notably, the multi

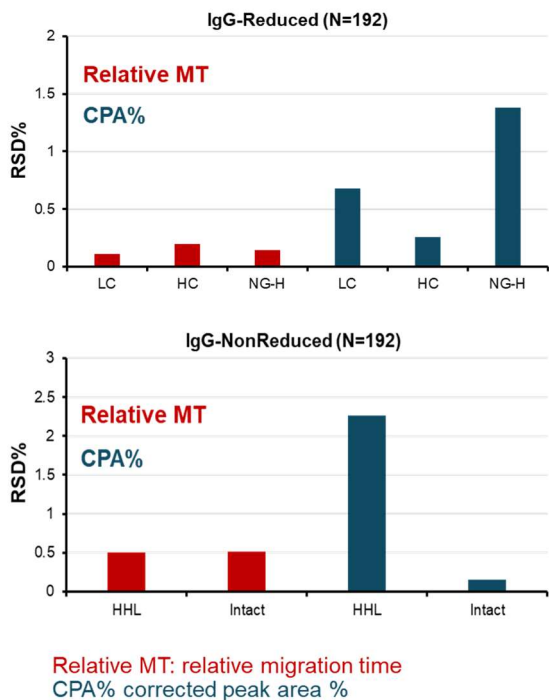


Figure 7. RSD% of lightning CE-SDS workflow for the major peaks of reduced and non-reduce IgG control standard.

capillary environment of the BioPhase 8800 system allowed to execute this study in only 6 days.

Table 2. Systematical study plan of NIST under reduced or non-reduced conditions.

# of Runs	Instrument	Person	Cartridge	Day
1	1	Analyst-1	3	
2	2	Analyst-2	2	1
3	3	Analyst-3	1	
4	1	Analyst-2	1	
5	2	Analyst-3	3	2
6	3	Analyst-1	2	
7	1	Analyst-3	2	
8	2	Analyst-1	1	3
9	3	Analyst-2	3	

Additionally, we used the original CE-SDS workflow as a control experiment but a reduced statistical sampling. In summary, 2 sequence analyses were performed using the same sample plate layout as Figure 2 for reduced and non-reduced NIST antibodies. Therefore, our control runs generated 48 data points for reduced or non-reduced conditions.

This comprehensive study systematically assessed factors that may impact MT, resolution and CPA% of major peaks of the NIST mAb.

Each bar graph shown in Figure 8 represents the average value of 24 data points collected with the original workflow or 216 data points (UV or LIF) collected by the lightning CE-SDS workflow with standard deviations as error bars. The average MT, CPA% and resolution values were very close between the original CE-SDS and the lightning CE-SDS workflow for all major peaks observed under reduced and non-reduced conditions. Most notably, the low CV% found for raw MT, CPA% and resolution was overall below 5%, indicating the robustness and reproducibility of the lightning workflow compared to the original for both detection modes. Additionally, the data also suggested that the duration of the separation is the same between the 2 workflows, facilitating method adoption. Similarly, the resolution between NG-H, HC peaks, HHL and the intact IgG peaks indicated the separation efficiency observed in the lightning CE-SDS workflow was not only maintained across the 216 data points but was equivalent to the original CE-SDS workflow.

Assessment of carryover: To check for any carryover issues due to the shortening of the rinsing steps specially when using LIF was also evaluated. We incorporated 6 blank injections in the plate layout where the separation of a blank sample always followed each sample separation. A closer look at the data from blank injections in Figure 9 revealed no carryover detected in the lightning CE-SDS workflow for both UV and LIF detection schemes.

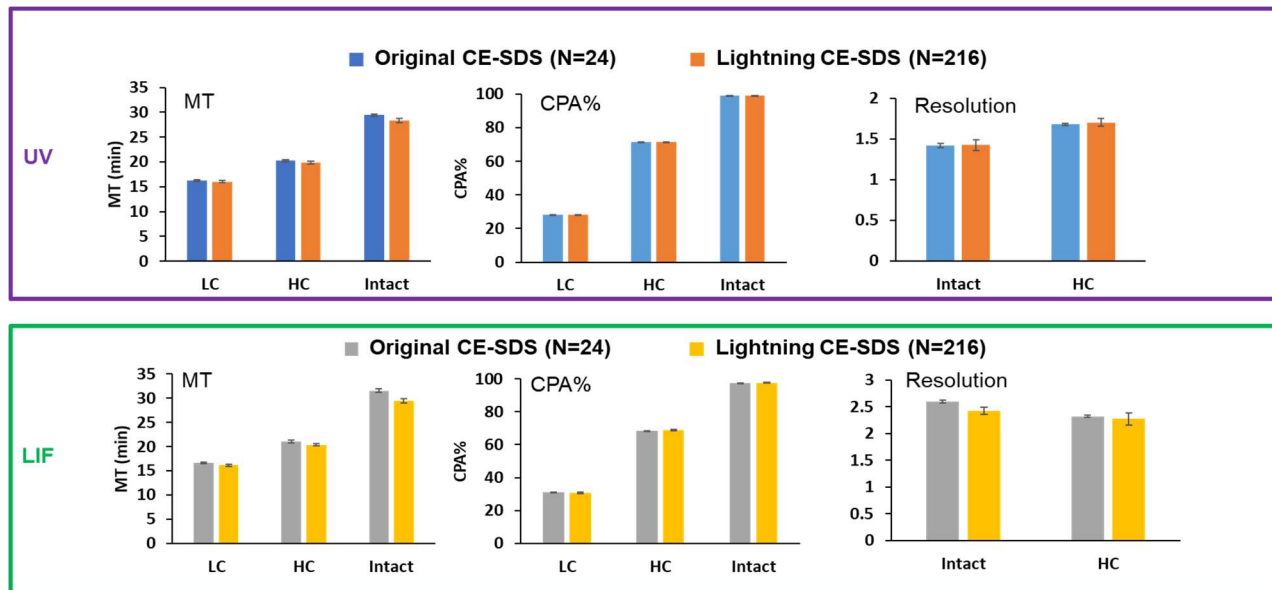


Figure 8. Attributes comparison (MT, CPA% and resolution) between original and lightning CE-SDS workflow (for both UV and LIF). The numbers in parentheses are the number of replicates. The error bars indicate the standard deviation.

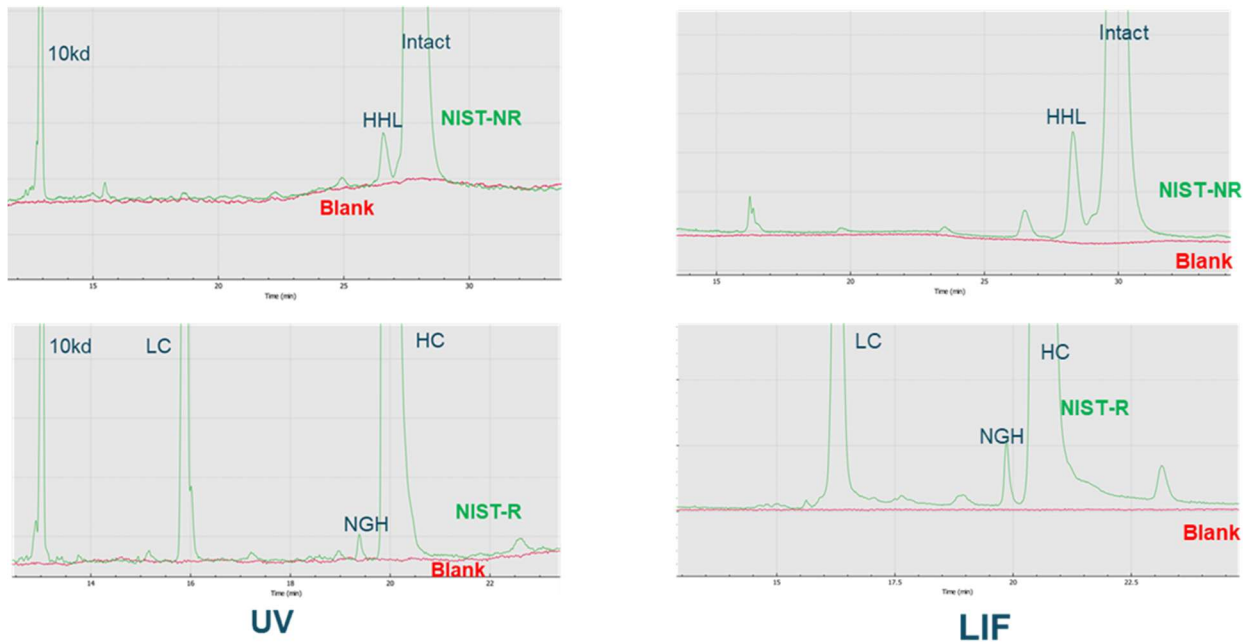


Figure 9. Electropherograms of non-reduced and reduced NIST mAb between sample and blank. The green trace was from sample at 1 mg/mL (UV) and 0.1 mg/mL (LIF). The red trace was from blank (SDS-MW sample buffer). Upper panels show results of non-reduced NIST mAb. Lower panels show results of reduced NIST mAb.

Finally, we systematically evaluated the impact of multiple factors such as, instrument, analyst, cartridge and capillaries on the attributes of resolution and CPA% of the lightning CE-SDS workflow. We isolated the results of each attribute so we could easily underscore how a factor such as, an instrument to instrument has any impact on the average of CPA% and

resolution between NG-H and HC. Figure 10 illustrates the average CPA% and resolution between NG-H and HC peaks when data is organized into instrument (green bars), analysts (blue bars), capillary cartridge (yellow bars), day (gray bars), injection (dark blue bars) and capillaries (orange bars). The error bars indicate the standard deviation of the replicates for each factor. Overall, this study revealed that the lightning CE-SDS

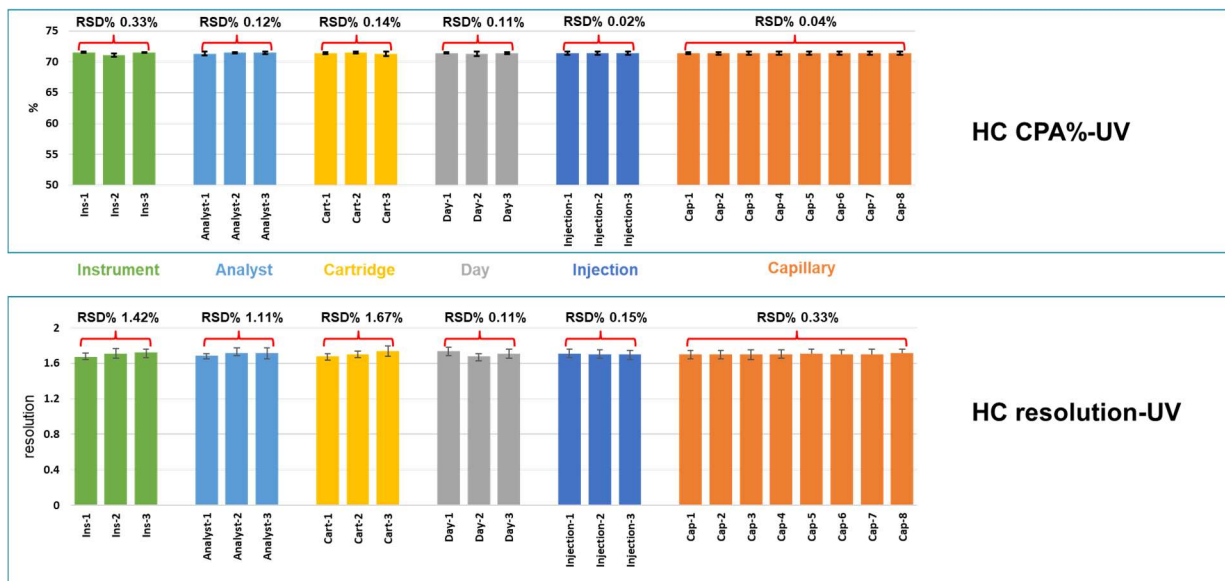


Figure 10. Attributes comparison under different conditions.

generated very reproducible data. For example, when considering instrument to instrument, we observed %RSD as low as 0.4% and below 2% for CPA% and resolution between NH-H and HC peaks, respectively. We also performed a similar analysis on other peaks under reduced and non-reduced conditions (data not shown) and reached the same conclusion.

When considering the 3 analysts as source of variation, our data showed minimum impact on all attributes considered in this study, indicating the robustness of the lightning CE-SDS workflow generating similar results as the SCIEX original CE-SDS workflow.

Conclusions

- The lightning CE-SDS increased the analysis speed up to 1.5 x compared to the original workflow, where 192 injections can be analyzed within 18 hours without the need to change reagent plates
- The reproducibility of the lightning CE-SDS workflow is remarkable with RSD% of < 1% and < 3% for calibrated MT and CPA%, respectively, for all major peaks of IgG standard
- The multi-factorial design of this experiment demonstrated that the lightning CE-SDS workflow is as accurate and precise as the original validated CE-SDS workflow with no carryover and loss of separation efficiency

References

1. Le H, Vishwanathan N, Jacob NM, Gadgil M, Hu WS. Cell line development for biomanufacturing processes: recent advances and an outlook. *Biotechnol Lett.* 2015 Aug;37(8):1553-64. (PMID: [25971160](#))
2. Yang X, Xu W, Dukleska S, Benchaar S, Mengisen S, Antochshuk V, Cheung J, Mann L, Babadjanova Z, Rowand J, Gunawan R, McCampbell A, Beaumont M, Meininger D, Richardson D, Ambrogelly A. Developability studies before initiation of process development: improving manufacturability of monoclonal antibodies. *MAbs.* 2013 Sep-Oct;5(5):787-94. (PMID: [23883920](#))
3. Rustandi RR, Washabaugh MW, Wang Y. Applications of CE SDS gel in development of biopharmaceutical antibody-based products. *Electrophoresis.* 2008 Sep;29(17):3612-20. (PMID: [18803223](#))

The SCIEX clinical diagnostic portfolio is For In Vitro Diagnostic Use. Rx Only. Product(s) not available in all countries. For information on availability, please contact your local sales representative or refer to <https://sciex.com/diagnostics>. All other products are For Research Use Only. Not for use in Diagnostic Procedures.

Trademarks and/or registered trademarks mentioned herein, including associated logos, are the property of AB Sciex Pte. Ltd. or their respective owners in the United States and/or certain other countries (see www.sciex.com/trademarks).

© 2022 DH Tech. Dev. Pte. Ltd. RUO-MKT-02-14803-A



Headquarters
500 Old Connecticut Path | Framingham, MA 01701 USA
Phone 508-383-7700
sciex.com

International Sales
For our office locations please call the division headquarters or refer to our website at sciex.com/offices



The Power of Precision

